Instability-induced dynamics of dark solitons

Dmitry E. Pelinovsky,* Yuri S. Kivshar, and Vsevolod V. Afanasjev
Optical Sciences Centre, The Australian National University, Canberra, Australian Capital Territory 0200 Australia
(Received 13 February 1996)

Nonlinear theory describing the instability-induced dynamics of dark solitons in the generalized nonlinear Schrödinger equation is presented. Equations for the evolution of an unstable dark soliton, including its transformation into a stable soliton, are derived using a multiscale asymptotic technique valid near the soliton instability threshold. Results of the asymptotic theory are applied to analyze dark solitons in physically important models of optical nonlinearities, including *competing*, *saturable*, and *transiting* nonlinearities. It is shown that in all these models dark solitons *may become unstable*, and two general (*bounded and unbounded*) scenarios of the instability development are investigated analytically. Results of direct numerical simulations of the generalized nonlinear Schrödinger equation are also presented, which confirm predictions of the analytical approach and display main features of the instability-induced dynamics of dark solitons beyond the applicability limits of the multiscale asymptotic theory. [S1063-651X(96)09707-3]

PACS number(s): 03.40.Kf, 42.60.Jf, 42.65.Jx

I. INTRODUCTION

Dark solitons are observed as localized intensity dips on a continuous-wave (cw) background, which are usually accompanied by a nontrivial phase change [1]. For a cubic (or Kerr-type) nonlinearity, *temporal dark solitons* have been predicted to exist in the normal dispersion regime of optical fibers and they have been already observed experimentally. These solitons are described by the integrable (cubic) nonlinear Schrödinger (NLS) equation [2,3]. Similarly, *spatial dark solitons* can propagate in nonlinear planar waveguides as stationary variations of the beam profile that do not diffract because diffraction is balanced by a defocusing nonlinearity. These self-trapped waves have been suggested as perfect self-induced optical waveguides to guide or steer another (probe) beam, thus manipulating light with light (see, e.g., [4]). Recent experimental observations of spatial dark solitons [4–8] and demonstration of their successful application for data coding and transmission in optical fibers [9] emphasize the importance of optical dark solitons for all-optical proceeding, switching, signal transmission, and other optical applications.

Optical dark solitons are of both fundamental and technological importance if they are stable under propagation. For temporal solitons, such stability has been proved in the framework of the cubic NLS equation, which is valid only for a weak (Kerr) nonlinearity. For spatial solitons, much higher powers are usually required, so that real optical materials demonstrate essentially non-Kerr behavior of the nonlinear refractive index for increasing light intensity. Typically, the nonlinear refractive index deviates from Kerr and, in particular, it saturates at higher intensities. Therefore, models with a more general form of the intensity-dependent refractive index must be employed to analyze dark solitons and their stability in such *non-Kerr materials*. In dimensionless units, these models can be reduced to the generalized NLS (GNLS) equation

$$2i\frac{\partial\Psi}{\partial t}+\frac{\partial^2\Psi}{\partial x^2}-F(|\Psi|^2)\Psi=0, \tag{1}$$

where $\Psi(x,t)$ is a slowly varying envelope of electric field and t and x have different meanings depending on the context of the physical problem under consideration. For example, for the stationary beam propagation in a dielectric waveguide, t and x stand for two spatial coordinates, longitudinal and transverse ones. Below, for simplicity, we call these variables ''time'' and ''coordinate,'' respectively.

Function $F(I)$ is proportional to the intensity-dependent change in the refractive index of an optical material, which is defined by the wave intensity $I\equiv|\Psi|^2$. For $F(I)=I$ the model (1) becomes integrable [2] and it supports conventional NLS dark solitons corresponding to a defocusing Kerr medium.

The generalized NLS equation (1) has been considered in many papers for analyzing the beam self-focusing and properties of spatial bright and dark solitons (see, e.g., Refs. [10–20] to cite a few). All types of non-Kerr nonlinearities that appear in the problems of nonlinear optics can be divided, generally speaking, into *three general classes*: (i) *competing nonlinearities*, e.g., focusing (defocusing) cubic and defocusing (focusing) quintic nonlinearity [11–14,17] (ii) *saturable nonlinearities* [15–19], and (iii) *transiting nonlinearities* [11,12].

Usually, the nonlinear refractive index of an optical material deviates from the linear (Kerr) dependence for larger light intensities. Nonideality of the nonlinear optical response is known for semiconductor (e.g., $Al_xGa_{1-x}As$, CdS, and $CdS_{1-x}Se_x$) waveguides and semiconductor-doped glasses (see, e.g., [21]). A larger deviation from the Kerr nonlinearity is observed for nonlinear polymers. For example, recently the measurements of a large nonresonant nonlinearity in single-crystal p-toluene sulfonate at 1600 nm [22] revealed a variation of the nonlinear refractive index with the input intensity, which can be modeled by *compet-*

*Permanent address: Department of Mathematics, Monash University, Clayton, Victoria 3168, Australia.

ing, cubic-quintic nonlinearity $\Delta n_{\rm nl}(I)=n_2 I+n_3 I^2$. This model describes a competition between self-focusing ($n_2>0$), at smaller intensities, and self-defocusing ($n_3<0$), at larger intensities.

Models with *saturable nonlinearities* are the most typical ones in nonlinear optics. For high power levels saturation of nonlinearity has been measured in many materials and consequently the maximum refractive index change has been reported (see, e.g., [23]). We do not linger on the physical mechanizms behind the saturation but merely note that it exists in many nonlinear media being usually described by phenomenological models introduced more than 25 years ago (see, e.g., Ref. [24]). The effective GNLS equation with saturable nonlinearity is also the basic model [18] to describe the recently discovered (1+1)-dimensional photovoltaic dark solitons in photovoltaic-photorefractive materials as $LiNbO_3$ [8]. Unlike the phenomenological models usually used to describe saturation of nonlinearity, for the case of photovoltaic solitons this model finds its rigorous justification (see, e.g., Refs. [18,19]).

Finally, *bistable solitons* introduced by Kaplan [11] usually require a special dependence of the intensity-dependent refractive index on light intensity, which should vary from one kind of the Kerr nonlinearity, for small intensities, to another kind with a different value of n_2, for larger intensities. This type of nonlinearity is known to support bistable dark solitons [12] as well. Unfortunately, examples of nonlinear optical materials with such dependences are not known yet, but the bistable solitons possess attractive properties useful for their possible futuristic applications in all-optical logic and switching devices.

The stability of bright solitons of the GNLS equation (1) has been extensively investigated for many years and the criterion for the soliton stability, as well as different scenarios of the instability-induced dynamics of bright solitons, has been found and analyzed analytically and numerically (for a review see, e.g., Ref. [25]). Recently, we have presented an asymptotic analytical approach [20] to this problem that not only describes, in a self-consistent manner, the long-term dynamics of unstable solitons but also reveals alternative scenarios of the evolution of unstable bright solitons of the GNLS equation.

In contrast to bright solitons, the general stability criterion for dark solitons of the GNLS equation (1) has not been understood until recently even in the framework of the linear stability analysis, and this issue created a lot of misunderstanding in the past. For example, we notice unsuccessful efforts to apply the known criterion for bright solitons to the case of dark solitons using, by a similarity, the so-called soliton complementary power (see, e.g., Refs. [12,17]). However, the recent analysis of instability of dark solitons and its application to a special (solvable) model of a saturable medium displayed a natural way to analyze such instability by means of the variational principle for dark solitons based on the renormalized soliton momentum [26].

In the present paper we investigate the problem of instability of dark solitons of the GNLS equation (1) in details and develop an analytical approach combining it with numerical simulations. The multiscale asymptotic method we employ here allows us to describe both *linear* (initial exponential growth of instability) and *nonlinear* (long-term evolution) regimes of the instability-induced dynamics of dark solitons in the GNLS equation. Our analytical results are rather general; they do not depend crucially on a particular choice of the nonlinear function $F(I)$. The only assumption for the asymptotic technique to be applied is a ''slow'' dynamics of the perturbed dark soliton; this assumption is always valid near the threshold of the soliton instability. However, in contrast to bright solitons of the GNLS equation, for dark solitons this situation is rather typical because for any type of the nonlinear function $F(I)$ dark solitons are always stable in the small-amplitude limit being described by an effective Korteweg–de Vries (KdV) equation (see, e.g., Ref. [1]). Therefore, if such an instability region exists, it occurs only for dark solitons of larger amplitudes and there exists at least one critical value of the soliton velocity separating stable and unstable stationary waves.

Investigating the instability of dark solitons of the GNLS equation (1), we follow the ideas of a multiscale asymptotic technique recently developed by us in Ref. [20] for *unstable bright solitons*. However, we would like to emphasize that the dynamics of an unstable dark soliton *differs drastically* from the corresponding dynamics of bright solitons.

Indeed, for the case of bright solitons there exist generally *three scenarios* of the instability-induced soliton dynamics, namely, the transition to and oscillations around a stable state, soliton decay into dispersive-diffractive waves, and soliton collapse, i.e., unlimited growth of the soliton amplitude. As shown in Ref. [20], all these scenarios can be predicted by an asymptotic approach that derives *adiabatic equations* for the soliton parameters resembling Newton's equations for an effective particle in a *conservative* system moving under the action of an external potential force.

For the case of dark solitons, as we demonstrate here, the instability development is accompanied by radiation. This radiation escapes the unstable dark soliton and propagates along the cw background inducing ''an effective dissipation'' to a dark soliton. As a result, an effective asymptotic equation governing the development of the dark soliton instability corresponds to the equation for an effective particle moving under the action of a nonlinear *dissipative* force. The role of radiation is very important and can be understood through the following simple physics. Indeed, when an unstable dark soliton evolves into a stable soliton, this should lead to a change of the phase difference across the dark soliton. Therefore, such a process is always accompanied by radiation that removes an excess of phase during the soliton transition, first locally, around the soliton core, but then propagating this phase difference to infinities.

The paper is organized as follows. In Sec. II we discuss properties of dark solitons of the GNLS equation (1) and present a summary of the multiscale asymptotic analysis that describes the instability-induced dynamics of a dark soliton near the instability threshold defined by the critical value of the soliton velocity. Details of the asymptotic analysis are given in Appendixes A–C. General features of equations of the asymptotic theory are discussed in Sec. III, where some analytical solutions are also found and analyzed. Using these analytical solutions as well as direct numerical simulations, in Secs. IV–VI we consider three typical, physically impor-

tant examples of the GNLS equation and describe characteristic scenarios of the instability-induced evolution of dark solitons. Finally, Sec. VII concludes the paper.

II. ASYMPTOTIC APPROACH TO SOLITON INSTABILITIES

A. Stationary soliton solutions

Dark solitons exist on a cw background wave of a constant amplitude $\Psi_b(t)=\sqrt{q}e^{i(\Omega t+R)}$, where $\Omega=-\frac{1}{2}F(q)$ and R is an arbitrary constant. The cw background is modulationally stable provided $F'(q)>0$ [27]. In this stable case, we are looking for solutions of Eq. (1) in the form $\Psi(x,t)=\psi(x,t)e^{i\Omega t}$ and consider the corresponding equation for the auxiliary function ψ,

$$2i\frac{\partial\psi}{\partial t}+\frac{\partial^2\psi}{\partial x^2}+[F(q)-F(|\psi|^2)]\psi=0. \tag{2}$$

Now, the dark soliton ψ_s is defined as a localized traveling-wave solution of Eq. (2),

$$\psi_s(\xi)=\Phi(\xi)e^{i\theta(\xi)}, \tag{3}$$

where $\xi=x-vt$ and two *real* functions $\Phi\equiv\Phi(\xi;v,q)$ and $\theta\equiv\theta(\xi;v,q)$ depend on two parameters, the soliton velocity v and the intensity q of the cw background. These functions satisfy the ordinary differential equations

$$\frac{d\theta}{d\xi}=v\left(1-\frac{q}{\Phi^2}\right), \tag{4}$$

$$\frac{d^2\Phi}{d\xi^2}+v^2\left(\Phi-\frac{q^2}{\Phi^3}\right)+[F(q)-F(\Phi^2)]\Phi=0. \tag{5}$$

Here we consider *nonzero boundary conditions* at both infinities $\Phi\to\sqrt{q}$ and $\theta\to R\pm\frac{1}{2}S_s$ as $\xi\to\pm\infty$, where S_s has the meaning of the total phase shift across the dark soliton. In addition, we classify all localized solutions on a nonvanishing background as *dark solitons* if $|\psi_s(\xi)|^2<q$ for any ξ and *bright-like dark solitons* otherwise (see also [14,27]). Although our theory can be applied to all types of localized solutions with nonzero asymptotes, we consider here only the case of conventional dark solitons, which have the minimum intensity $I_{\min}$ lower than the background intensity q.

The solution (3)–(5) describes a dark soliton with the velocity v, which propagates on the (stationary) cw background $\psi_b=\sqrt{q}e^{iR}$; the dark soliton modifies locally the intensity q and the phase R of the background. However, we can also generalize this particular solution and consider the dark solitons propagating on the moving cw background $\psi_b=\sqrt{q}e^{i[kx-(k^2/2)t+R]}$. In this case, a more general dark soliton solution follows from a simple Galilei transformation

$$\widetilde{\psi}(x,t)=\psi(x',t')e^{ik[x'+(k/2)t']}, \tag{6}$$

where $x'=x-kt$, $t'=t$, and functions $\widetilde{\psi}$ and ψ satisfy the same GNLS equation (2) in the corresponding variables. Applying the transformation (6) at $k=v$, we can construct the (stationary) dark soliton solution located at the cw background moving with the phase velocity $v_b=-/2$. We shall use this representation of the dark soliton solutions in some numerical simulations of Eq. (2) described in Secs. IV–VI below.

As follows from Eq. (5), the solution for a dark soliton is defined by two parameters v and q. Under the action of perturbations growing due to the soliton instability, the velocity v becomes a varying quantity that can be used to characterize the dark soliton as an effective particle. On the other hand, in spite of the fixed boundary conditions at infinities, some *local variations* of the background intensity q in the vicinity of the soliton are still possible and these variations appear as radiative waves or additional shallow dark solitons escaping the unstable dark soliton.

In order to describe the instability-induced dynamics of a dark soliton in the GNLS equation (2), we introduce the important integral characteristics calculated for the soliton solution (3). Following [28,29], we use the following invariants: complementary power N, renormalized momentum P, and renormalized Hamiltonian H, and calculate them for the stationary soliton solution (3) (we denote these values by the indices s),

$$N_s(v,q)=\frac{1}{2}\int_{-\infty}^{+\infty}(|\psi_s|^2-q)d\xi=\frac{1}{2}\int_{-\infty}^{+\infty}(\Phi^2-q)d\xi, \tag{7}$$

$$P_s(v,q)=\frac{i}{2}\int_{-\infty}^{+\infty}\left(\psi_s^*\frac{d\psi_s}{d\xi}-\psi_s\frac{d\psi_s^*}{d\xi}\right)\left(1-\frac{q}{|\psi_s|^2}\right)d\xi$$
$$=-v\int_{-\infty}^{+\infty}\frac{(\Phi^2-q)^2}{\Phi^2}d\xi, \tag{8}$$

$$H_s(v,q)=\frac{1}{2}\int_{-\infty}^{+\infty}\left\{\left|\frac{d\psi_s}{d\xi}\right|^2+\int_q^{|\psi_s|^2}[F(I)-F(q)]dI\right\}d\xi$$
$$=\frac{1}{2}\int_{-\infty}^{+\infty}\left\{\left(\frac{d\Phi}{d\xi}\right)^2+v^2\frac{(\Phi^2-q)^2}{\Phi^2}\right.$$
$$\left.+\int_q^{\Phi^2}[F(I)-F(q)]dI\right\}d\xi. \tag{9}$$

The physical meaning of these invariants has been clarified in Ref. [28]. Importantly, each of these invariants is constructed as a difference between the corresponding (standard) integral of motion of the GNLS equation (2) and a contribution from the cw background; the latter is conserved independently provided that the boundary conditions at infinities are fixed (see discussions in Ref. [28]). Thus, if a cw background has ''a defect'' in the form of a hole described by a dark soliton, the renormalized invariants just correspond to the hole itself excluding the background. As follows from the analysis presented below, the renormalized momentum (8) is the most important invariant of a dark soliton (see also Ref. [28]). In addition, we can find the analytical expression for the total phase shift S_s of the background wave across the dark soliton,

$$S_s(v,q)=v\int_{-\infty}^{+\infty}\left(1-\frac{q}{\Phi^2}\right)d\xi. \tag{10}$$

There exist several remarkable relations between the soliton invariants (7)–(10). First, we can find relations for the variations of the renormalized momentum P_s and energy H_s,

$$v\frac{\partial P_s}{\partial v}+\frac{\partial H_s}{\partial v}=0, \tag{11}$$

$$v\left(\frac{\partial P_s}{\partial q}-S_s\right)+\left(\frac{\partial H_s}{\partial q}+F'(q)N_s\right)=0, \tag{12}$$

where $F'(q)\equiv dF/dq$. These relations represent a variational principle for dark solitons already established in Refs. [28,29] and can be used for characterizing a variation of the soliton parameters in the so-called *adiabatic approximation* [28].

Next, we notice that the renormalized momentum can be expressed through the complementary power N_s and the total phase shift S_s,

$$P_s=qS_s-2vN_s. \tag{13}$$

The relation (13), together with Eqs. (11) and (12), leads to two other equations

$$\frac{\partial P_s}{\partial v}+2N_s=q\frac{\partial S_s}{\partial v}-2v\frac{\partial N_s}{\partial v}, \tag{14}$$

$$\frac{\partial P_s}{\partial q}-S_s=v\frac{\partial S_s}{\partial v}-\frac{2c^2}{q}\frac{\partial N_s}{\partial v}, \tag{15}$$

where we have introduced the velocity of linear waves propagating along the cw background,

$$c=\sqrt{\frac{q}{2}F'(q)}. \tag{16}$$

The soliton velocity v is always less than this limiting value, $|v|<c$.

Thus, using Eqs. (11), (14), and (15), we can express the three invariants calculated for the stationary soliton solution (3), i.e., the soliton complementary power, the soliton renormalized energy, and the total phase shift, through only one, the soliton renormalized momentum. Therefore, the instability-induced dynamics of a dark soliton is finally governed by a unique equation for the only parameter, the soliton velocity v.

B. Equation for soliton velocity

We assume that the stationary dark soliton (3) of the GNLS equation (2) can become unstable with respect to small perturbations in a certain region of parameters of the function $F(I)$ and for certain values of the soliton velocity v. Our main purpose is to describe analytically the evolution of an unstable dark soliton deriving from the GNLS equation (2) a simplified ordinary differential equation for the slowly varying soliton velocity and determining the radiation fields generated during the soliton evolution. Such a reduction can be done in the framework of the perturbation theory for solitons [30] if a change of the soliton parameters is slow in time. It is obvious that soliton instability develops slowly

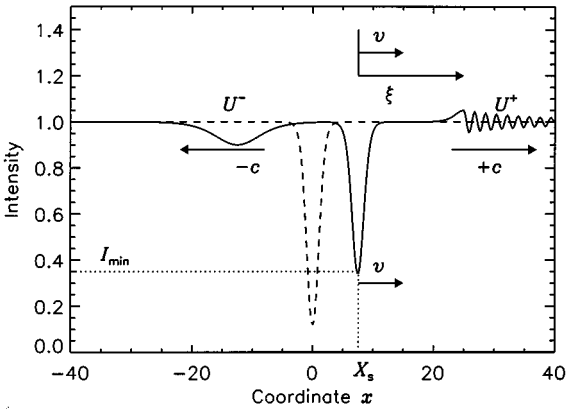

FIG. 1. Schematic presentation of the instability-induced evolution of a dark soliton for a bounded scenario, when a transformation of an unstable dark soliton is observed. The initial (unstable) dark soliton is shown by a dashed curve and two stable (created after the splitting) dark solitons and radiation fields emitted during the instability development are shown by a solid curve. Notations are explained in the text.

near the instability threshold, which is defined by the equation $\partial P_s/\partial v|_{v=v_{\rm cr}}=0$ (see [26]), where $v_{\rm cr}$ is a critical value for the dark soliton velocity. Furthermore, we suppose that the amplitude of instability-induced perturbations remains small for an extended time interval and the localized wave is close to a dark soliton ψ_s with slowly (adiabatically) varying parameters. Therefore, we can introduce a small parameter ϵ, which characterizes a small perturbation of the unstable dark soliton, and look for solutions ψ to Eq. (2) in the form of the asymptotic (multiscale) expansion

$$\psi=\{\psi_s(\xi;v,q)+\epsilon\psi_1(\xi;v,q;X,T) +\epsilon^2\psi_2(\xi;v,q;X,T)+O(\epsilon^3)\}e^{iR(X,T)}, \tag{17}$$

where

$$\xi=x-\frac{1}{\epsilon}X_s(T),\quad X_s(T)=\int_0^T v(T')dT',\quad X=\epsilon x,\quad T=\epsilon t,$$

and $\epsilon\ll 1$. Here $v(T)$ $(v>0)$ and $R(X,T)$ describe the slowly varying soliton velocity and local phase of the background wave near the soliton, respectively, X and T stand for ''slow'' spatial and temporal variables, and $X_s(T)$ is the coordinate of the soliton center (where the intensity reaches its minimum value $I_{\rm min}$) with respect to the X axis (see Fig. 1).

Using the asymptotic expansion (17) and the form of the stationary soliton solutions $\psi_s(\xi)$ given by Eqs. (3)–(5), in Appendix A we present the analysis of the first-order perturbation correction ψ_1. This correction can be found as a solution of a linear inhomogeneous equation [see Eq. (A1) in Appendix A]. It follows from this analysis that the function ψ_1 varies along two characteristic scales of ξ, which can be treated as the *inner* interval with respect to the core of the solitary wave (see Fig. 1) when $\xi\sim O(1)$ and $X\to X_s(T)$ and the *outer* interval, for which $\xi\to\pm\infty$ and $X-X_s(T)\sim O(1)$. Asymptotic expansions for each interval should be analyzed separately.

Generally speaking, solutions to the linear inhomogeneous equations may diverge exponentially along the inner interval as $\xi\to\infty$ (see, e.g., discussion of the asymptotic technique in Ref. [20]). Such divergences usually break down the asymptotic expansion procedure. However, in the vicinity of the instability threshold, where $\partial P_s/\partial v\sim O(\epsilon)$, the first-order correction ψ_1 can be shown to be free of exponentially diverging terms (see Appendix A). Therefore, we can find this correction in an implicit form [see Eq. (A3) in Appendix A] and then proceed with the analysis of the second-order approximation where a bounded solution for the second-order perturbation correction ψ_2 should be found. In this way, the function ψ_2 does not have exponentially diverging terms if the velocity of the perturbed dark soliton satisfies a certain differential equation, *solvability condition* [see Eq. (19) below]. In Appendix B we present derivation of this equation from the balance equations for two conserved quantities, namely, renormalized momentum and Hamiltonian of the GNLS equation (2). It can be shown that the asymptotic approach that involves invariants is completely equivalent to a direct multiscale analysis. Next we proceed to the analysis of the instability-induced evolution of the field in the outer interval of the asymptotic expansions. As follows from Eq. (A5) of Appendix A, the first-order correction ψ_1 grows proportionally to ξ as $\xi\to\pm\infty$. Therefore, this perturbation is still secular, but this secular growth is power law instead of exponential. It is known (see, e.g., [31]) that such algebraically divergent terms of multiscale asymptotic expansions corresponds to radiation emitted by the soliton. Therefore, in the region where the localized wave vanishes, we seek solutions to the GNLS equation (2) in the asymptotic form

$$\psi_\infty^\pm=\lim_{\xi\to\pm\infty}\psi=\Phi^\pm(X,T)\exp[i\Theta^\pm(X,T)], \qquad (18)$$

where

$$|\psi_\infty^\pm|^2=(\Phi^\pm)^2=q+\epsilon U^\pm(X,T)+O(\epsilon^2),$$

$$\Theta^\pm=\Theta_0^\pm(X,T)+O(\epsilon).$$

This asymptotic expansion is analyzed in Appendix C, where we show that the radiation fields $U^\pm$ outside the soliton region are presented by a superposition of two linear waves propagating with the velocities $\pm c$, i.e., $U^\pm=U^\pm(X\mp cT)$ (see Fig. 1). A profile of the radiation fields generated by the perturbed dark soliton can be found explicitly [see Eqs. (25) and (26) below] by matching the asymptotic series (17) and (18) by a formal extension $\epsilon\xi=X-X_s(T)$.

Now we present the main asymptotic equations of the multiscale perturbative approach in an explicit form. Using the results given by Eqs. (14), (15), (A11), (A12), (C5), and (C6), we rewrite the equation for the renormalized momentum P [see Eqs. (B6) and (B7) in Appendix B] as a differential equation for the soliton velocity $v(T)$,

$$\frac{d}{dT}\left[\frac{1}{\epsilon}P_s(v,q)+M_s(v,q)\frac{dv}{dT}\right]=K_s(v,q)\left(\frac{dv}{dT}\right)^2, \quad (19)$$

where P_s is the renormalized momentum calculated for the dark soliton according to Eq. (8) and the coefficients are defined as

$$M_s(v,q)=\left[\frac{2c}{q}\left(\frac{\partial N_s}{\partial v}\right)^2+\frac{q}{2c}\left(\frac{\partial S_s}{\partial v}\right)^2\right] \qquad (20)$$

and

$$K_s(v,q)=\frac{1}{(c^2-v^2)}\left[\frac{2cv}{q}\left(\frac{\partial N_s}{\partial v}\right)^2+2c\frac{\partial N_s}{\partial v}\frac{\partial S_s}{\partial v}+\frac{vq}{2c}\left(\frac{\partial S_s}{\partial v}\right)^2\right]. \qquad (21)$$

Equations (19)–(21) present one of the main results of our asymptotic analysis.

On the other hand, similar calculations show that the equation for the Hamiltonian [see Eqs. (B8) and (B9) in Appendix B] leads to the other differential equation for $v(T)$,

$$\frac{d}{dT}\left[\frac{1}{\epsilon}H_s(v,q)-vM_s(v,q)\frac{dv}{dT}\right]=L_s(v,q)\left(\frac{dv}{dT}\right)^2, \quad (22)$$

where H_s is the soliton renormalized energy defined by Eq. (9) and

$$L_s(v,q)=-\frac{c}{(c^2-v^2)}\left[\frac{2c^2}{q}\left(\frac{\partial N_s}{\partial v}\right)^2+2v\frac{\partial N_s}{\partial v}\frac{\partial S_s}{\partial v}+\frac{q}{2}\left(\frac{\partial S_s}{\partial v}\right)^2\right]. \qquad (23)$$

We note that Eqs. (19) and (22) are *self-consistent* because it is easy to verify that $L_s(v,q)=-M_s(v,q)-vK_s(v,q)$. Besides, we can immediately see that the variational principle for dark solitons (see discussions in Ref. [28]), which is expressed in the adiabatic (zeroth-order) approximation by Eq. (11), is still valid when a dark soliton evolves under the action of the instability-induced perturbations. Indeed, it follows from Eqs. (19) and (22) that the first-order variations of the renormalized momentum δP and Hamiltonian δH of a perturbed dark soliton are related by the equation

$$v\,\delta P+\delta H=0. \qquad (24)$$

However, neither momentum nor Hamiltonian of the perturbed dark soliton is a conserved quantity and this leads to an essentially dissipative character of the instability-induced dynamics of unstable dark solitons. Such a dissipative dynamics of the dark soliton instability is explained by generation of the radiation fields propagating away from the perturbed dark soliton to the right and to the left. The profile of the radiation fields is given by the boundary condition (C4) estimated at the soliton position $X=X_s(T)$. Using the previous analysis, we can rewrite (C4) in the explicit form

$$U^\pm=\zeta_\pm(v,q)\frac{dv}{dT}\ \text{ at } X=X_s(T), \qquad (25)$$

where

$$\zeta_\pm(v,q)=-\frac{1}{c(c\mp v)}\left(c\frac{\partial N_s}{\partial v}\pm\frac{q}{2}\frac{\partial S_s}{\partial v}\right). \qquad (26)$$

Finally, we show that the perturbed dark soliton and two radiation fields represent a complete system because the total momentum and energy are conserved quantities. Indeed, let us introduce the total momentum of the wave field according to the expression

$$P_{\rm tot}=P+\epsilon\left\{\int_{-\infty}^{X_s(T)}p_\infty^-(X+cT)dX+\int_{X_s(T)}^{+\infty}p_\infty^+(X-cT)dX\right\}, \tag{27}$$

where P is the renormalized momentum of the perturbed dark soliton given by Eq. (B7) in Appendix B and $p_\infty^\pm$ are the renormalized momentum densities calculated for the radiation fields. The leading order of these densities can be found by substituting Eq. (18) into Eq. (B2) defined in Appendix B,

$$p_\infty^\pm=-U^\pm\frac{\partial\Theta_0^\pm}{\partial X}=\mp\left(\frac{c}{q}\right)(U^\pm)^2, \tag{28}$$

where we have used the result (C3) from Appendix C. Using Eqs. (25) and (26), we can rewrite Eq. (19) in the form

$$\frac{1}{\epsilon}\frac{dP}{dT}=\frac{c(c-v)}{q}(U^+)^2\Big|_{X=X_s(T)}-\frac{c(c+v)}{q}(U^-)^2\Big|_{X=X_s(T)}. \tag{29}$$

By virtue of Eq. (29) we prove that the derivative of $P_{\rm tot}$, defined by Eq. (27), with respect to T is identically equal to zero. Similarly, we can show that the total Hamiltonian of the perturbed dark soliton and two radiation fields is also a conserved quantity. This means that the equation for the soliton velocity and the radiation fields give *a complete description* of the instability-induced evolution of a dark soliton near the instability threshold.

The asymptotic equations (19) or (22) cannot be generally integrated. Nevertheless, they describe a rather simple scenario of the dark soliton instability and related evolution of the radiation fields (25). The general features of this dynamics are analyzed in Sec. III, whereas Secs. IV–VI are devoted to applications of our general approach to some particular types of the GNLS equation (2) that are important in the theory of optical dark solitons.

III. ANALYSIS OF ASYMPTOTIC EQUATIONS

A. Criterion of linear instability

First we consider a linear approximation of the asymptotic equation (19) substituting $v=v_0+v_1e^{\lambda T}$, where v_0 is the initial velocity of the unperturbed dark soliton and v_1 is its small deviation caused by an initial perturbation. Neglecting nonlinear terms in Eq. (19), we find the eigenvalue λ,

$$\lambda=-\frac{1}{\epsilon M_s(v_0,q)}\left(\frac{\partial P_s}{\partial v}\right)\Big|_{v=v_0}. \tag{30}$$

The result (30) can be treated as the first-order approximation to the eigenvalue of the linear stability problem, which is valid only provided that $\partial P_s/\partial v|_{v=v_0}\sim O(\epsilon)$. This implies that the value v_0 of the velocity of the unperturbed dark soliton should be chosen near the critical value $v_{\rm cr}$ where the derivative $\partial P_s/\partial v$ vanishes. The result (30) confirms the general criterion of the dark soliton instability discussed in Ref. [26] and proves that dark solitons become unstable provided $\partial P_s/\partial v|_{v=v_0}<0$ [we notice that the coefficient $M_s(v_0,q)$ is always positive; see the definition in Eq. (20)]. Inside the instability region there exists a real positive eigenvalue λ that determines the growth rate of exponentially growing perturbations. Although a mathematically rigorous proof of the general linear stability theorem for dark solitons is still an open problem, the linear analysis implies that *all dark solitons with negative slope of the renormalized momentum $P_s(v)$ defined by Eq. (8) are unstable* [32]. Note that this criterion is *different* from that for bright solitons of the GNLS equation, which become unstable if the derivative of the soliton power N_s on the soliton propagation constant β (or frequency) is negative, i.e., $dN_s/d\beta<0$ (see, e.g., [25]).

Now we analyze the general conditions when the instability of dark solitons can occur. First consider the small-amplitude limit, when $|v|\to c$. In this case, as follows from Eqs. (27) and (28), the renormalized momentum of the small-amplitude wave fields is asymptotically given by

$$P^\pm=\mp\frac{\epsilon c}{q}\int_{-\infty}^{+\infty}(U^\pm)^2dX. \tag{31}$$

Using the analytical approach discussed in Ref. [1] (see also Appendix C), we can reduce the GNLS equation (2) to a pair of uncoupled KdV equations describing long-wave small-amplitude perturbations of the continuous-wave background [see Eqs. (C7)]. The soliton solutions to these equations have the well-known form of the KdV solitons,

$$U_s^\pm=-\frac{12\epsilon\kappa^2}{\nu}{\rm sech}^2\left[\kappa\left(X\mp cT\pm\frac{\kappa^2}{2c}\tau\right)\right], \tag{32}$$

where κ determines the soliton amplitude. These expressions present the so-called small-amplitude approximation to the stationary soliton solutions of the GNLS equation (2). Note that this approximation fails for $\nu\to0$ when the quadratic nonlinear term in the KdV equations vanishes. However, in this paper we consider the case when Eq. (2) supports only conventional dark solitons, which are described by the functions $U_s^\pm<0$ for any X. The corresponding KdV equations (C7) derived in this case always have a positive coefficient ν.

It is known that in the framework of the KdV equation solitons are always stable. This result can be verified directly with the help of Eq. (31) by evaluating the slopes of the renormalized soliton momenta $P^\pm$ with respect to the soliton velocity $v=\pm[c-\epsilon^2\kappa^2/2c+O(\epsilon^4)]$,

$$\frac{1}{\epsilon}\left(\frac{\partial P^\pm}{\partial v}\right)\Big|_{v\to\pm c}\to\frac{576c^2\kappa}{q\nu^2}.$$

Therefore, the important conclusion is the following: Small-amplitude (shallow) dark solitons of the GNLS equation (2) are *always stable* and the instability can occur either for intermediate values of the soliton velocity v or in the limit of black soliton corresponding to $v\to0$. The former case is not generic and depends strongly on the type of nonlinearity involved (see, as an example, the case of transiting nonlinear-

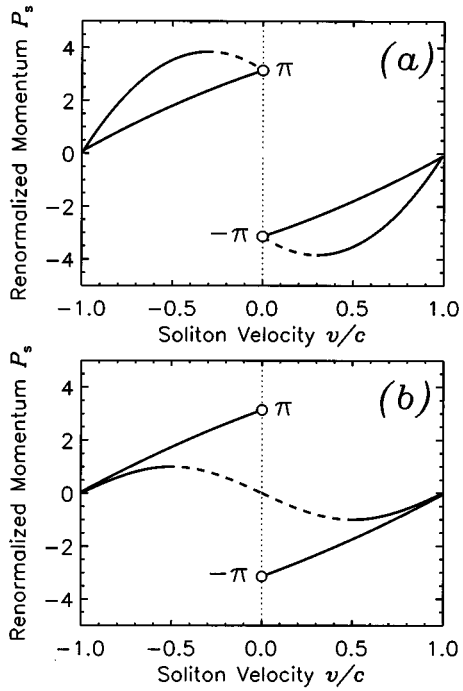

FIG. 2. Schematic presentation of the renormalized momentum $P_s(v)$ of the dark soliton for two distinct cases: (a) the minimum intensity always vanishes when $V\to 0$ and (b) the minimum intensity may become finite for $V\to 0$. In both cases the negative slope indicates unstable dark solitons.

ity discussed in Sec. VI below). In the latter case, some general results can be obtained independently of the type of nonlinearity supporting dark solitons (see also two examples in Secs. IV and V below).

Therefore, we analyze now the limit of small velocities $v\to 0$ and calculate again the slope $\partial P_s/\partial v$ defined by Eq. (14). Because N_s, S_s are always negative for conventional dark solitons [see Eqs. (7) and (10) provided that $\Phi^2<q$ and $v>0$] we note that the slope $\partial P_s/\partial v$ *can become negative* in the limit $v\to 0$ only if

$$\left(\frac{\partial S_s}{\partial v}\right)\Big|_{v=0} < \frac{2}{q}N_s\Big|_{v=0} < 0. \tag{33}$$

The result (33) gives the necessary condition for instability of dark solitons to occur. For many models, the total phase shift S_s is a monotonic function rising from the limiting value $-\pi$ at $v\to 0$ (''black'' soliton) to zero at $v\to c$ (small-amplitude or ''gray'' solitons). For example, this situation is typical for the Kerr and power-law nonlinearity $F\sim I^p$ as well as for the generalized Kerr model with the nonlinear function $F(I)=I+\beta I^2$, $\beta>0$ (see [17]). For these models the slope $\partial S_s/\partial v$ is always positive and instabilities of dark solitons are not observed. However, for other models the instability of dark solitons does take place and it is observed for small velocities when the change of the soliton phase becomes nonmonotonic.

In general, the instability for small velocities corresponds to two distinct types of dependences of the renormalized momentum P_s vs v [see Figs. 2(a) and 2(b)]. In the first case, a dark soliton always has a zero intensity at $v=0$, so that the renormalized momentum $P_s(v)$ is not defined at $v=0$ approaching π for $v\to 0-$ or $-\pi$ for $v\to 0+$, as shown in Fig. 2(a). In this case, the black soliton corresponds to the phase jump π and instability occurs when the function $P_s(v)$ displays a negative slope [see Fig. 2(a), dashed curve]. The other, qualitatively different, case is presented in Fig. 2(b) and corresponds to the situation when a black soliton, i.e., a soliton at $v=0$, does not reach the zero minimum intensity. This is possible, for example, when nonlinearity is self-focusing for small intensities (see Sec. IV). Then the black soliton with nonzero minimum intensity has no phase jump across the localized region and therefore $P_s(0)=0$. This kind of ''phase transition'' corresponds to a sudden structural change of the soliton renormalized momentum, as shown in Fig. 2(b); and the appearence of the negative slope indicating unstable solitons.

B. Nonlinear regime: Analytical solutions

Now we analyze the asymptotic equations (19) and (25) that describe the nonlinear dynamics of an unstable dark soliton and radiation fields emitted. It is clear that due to the factor $1/\epsilon$ in Eq. (19) our asymptotic approach is valid only in a small-velocity region near the critical velue $v_{\rm cr}$. Therefore, we apply a small-amplitude (but still nonlinear) approximation substituting $v=v_0+\epsilon V(T)$, in order to integrate Eq. (19) and reduce it to the form

$$M_s(v_0,q)\frac{dV}{dT}+\frac{1}{\epsilon}\left(\frac{\partial P_s}{\partial v}\right)\Big|_{v=v_0} V+\frac{1}{2}\left(\frac{\partial^2 P_s}{\partial v^2}\right)\Big|_{v=v_0} V^2=0. \tag{34}$$

This equation resembles the motion equation of an effective particle of mass M_s and velocity V under the action of a nonlinear dissipative force. Therefore, the instability-induced dynamics of a dark soliton may demonstrate two types of scenarios, bounded and unbounded ones.

1. Soliton evolution: Bounded scenario

The type of the instability scenario depends on a sign of the initial perturbation and the particular form of the dependence $P_s(v)$. We consider the case when dark solitons of smaller velocity are linearly unstable, while small-amplitude solitons with the velocities close to the limiting velocity c are stable. Therefore, for this type of the functions $P_s(v)$ the derivative $(\partial^2 P_s/\partial v^2)|_{v=v_0}$ in Eq. (34) is positive [we recall that $P_s<0$ for $v>0$ see Eq. (8)]. Then, as follows from Eq. (34), any perturbation with the positive change of the velocity, i.e., $V(0)\equiv V_0>0$, leads to a bounded scenario of the dark soliton instability when such a perturbation increases the soliton velocity v and decreases its amplitude, which is proportional to $(q-I_{\rm min})^{1/2}$ (see Fig. 1). This process corresponds to a transformation of an unstable dark soliton into a stable soliton of larger velocity. Such a transformation is described by a simple bounded solution of Eq. (34),

$$V=\frac{V_0V_f}{(V_f-V_0)e^{-\lambda T}+V_0}, \tag{35}$$

where λ is defined by Eq. (30) ($\lambda>0$), V_0 is the initial deviation of the velocity of the unstable dark soliton, and V_f, defined as

$$V_f=-\frac{2}{\epsilon}\left(\frac{\partial P_s}{\partial v}\right)\Bigg|_{v=v_0}\Bigg/\left(\frac{\partial^2 P_s}{\partial v^2}\right)\Bigg|_{v=v_0}, \tag{36}$$

is the change of the velocity corresponding to a stable soliton. This result is valid only if the renormalized momentum of the perturbed dark soliton is a conserved quantity during the soliton transformation. However, it follows from Sec. II B that this quantity does not conserve beyond the quadratic approximation and its variation is described asymptotically by Eq. (19). Using the approximate solution (35), we can estimate the difference ΔP between the value of the renormalized momentum P_f for the final stable dark soliton and that for the initial (unstable) soliton P_0. This difference can be calculated directly from Eq. (19) as

$$\Delta P=\epsilon\int_{-\infty}^{+\infty}K_s(v,q)\left(\frac{dv}{dT}\right)^2dT=\frac{\epsilon^3\lambda V_f^2}{6}K_s(v_0,q), \tag{37}$$

where the coefficient K_s is defined in Eq. (21). We note that this coefficient can have, in general, *an arbitrary sign* and therefore transitions from unstable to stable dark solitons can lead to either an increase or decrease of the value of the soliton renormalized momentum. As a matter of fact, the sign of the momentum change is determined by a balance between the radiation field U^+ propagating in the same direction as the perturbed dark soliton and the field U^- propagating to the opposite direction (see Fig. 1). Indeed, as follows from Eq. (29), the copropagating wave U^+ always leads to an increase of the renormalized momentum of the perturbed dark soliton, while the counterpropagating radiation wave U^- always leads to a decrease of the momentum. As will be shown for the particular cases discussed in Secs. IV and V, both these phenomena can actually take place for different types of GNLS equation.

2. Structure of radiation

As we have shown in Sec. II B, a change of the renormalized momentum of the perturbed dark soliton is caused by radiation fields, which are asymptotically described by Eq. (25) at the soliton position $X=X_s(T)$. Using the analytical solution (35) defined througout the T axis, we can find explicitly the profile of the radiation fields in the weakly nonlinear (quadratic) approximation when Eq. (34) is still valid and $X_s(T)$ is given approximately by $X_s=v_0T+O(\epsilon)$. This allows us to find the exact results for the radiation fields $U^\pm\to\epsilon U^\pm$, where

$$U^\pm=\frac{\lambda V_f}{4}\zeta_\pm(v_0,q)\,\mathrm{sech}^2\left[\frac{\lambda}{2(c\mp v_0)}(X\mp cT)\right]. \tag{38}$$

Radiation fields (38) coincide, with an accuracy of the amplitude factor, with the sech^2-type profile of the stationary dark soliton solutions to the GNLS equation (2) in the small-amplitude approximation [i.e., the KdV soliton; see Eq. (32)]. Moreover, the evolution of the radiation field given by Eq. (38) was shown in Appendix C to obey asymptotically the KdV equations (C7) with positive value of the coefficient ν. It is well known (see, e.g., Ref. [33]) that the sech^2-type initial pulse in the KdV equation (C7) can generate solitons only if the pulse amplitude is negative. In the opposite case, i.e., when the input amplitude of the localized pulse is positive, the initial profile (38) transforms into linear dispersive waves [33], which, in our problem, asymptotically disperse on the cw background $I=q$.

Amplitudes of the radiation fields (38) are proportional to the coefficients $\zeta_\pm(v_0,q)$, which are defined by Eq. (26). Let us evaluate the signs of these coefficients in the limiting case $v_0\to0$. In this limit, we find from Eqs. (26) and (14) that

$$\zeta_\pm=\mp\frac{1}{c^2}N_s(v_0=0,q)+O(v_0).$$

However, the soliton complimentary power $N_s(v,q)$ is always negative and therefore, in the limit $v_0\to0$, the coefficient ζ_+ is *positive*, while the coefficient ζ_- is *negative*. Moreover, we can show that the sign of the coefficient ζ_- remains unchanged throughout the instability region so that the counterpropagating radiation field, described by the function U^-, should always generate an additional (shallow) dark soliton as a result of the transformation of the primary unstable dark soliton. On the other hand, the radiation field, described by the function U^+, decays into dispersive waves if $\zeta_+(v_0,q)>0$ or it can also produce an additional dark soliton provided that $\zeta_+(v_0,q)<0$.

Using Eqs. (31) and (38), we can calculate the parts $P^\pm$ of the renormalized momentum of the perturbed dark soliton that are taken by the radiation fields generated due to the development of the soliton instability. The result is

$$P^\pm=\mp\frac{\epsilon^3c\lambda(\Delta V)^2(c\mp v_0)}{6q}\zeta_\pm^2(v_0,q). \tag{39}$$

It is easy to verify that the conservation of the total momentum leads to the balance $\Delta P+P^++P^-=0$. Thus we arrive at the conclusion that near the instability threshold the perturbation, which initially *decreases* the amplitude of the dark soliton, induces *a splitting of the unstable dark soliton* into (at least two) counterpropagating (stable) solitons of larger velocities and linear dispersive waves (or, in exceptional cases, an additional soliton) in front of the dark soliton, Fig. 1. The relation between these three components defines the general character of the instability-induced soliton dynamics.

3. Soliton evolution: Unbounded scenario

Finally, we discuss the other type of initial perturbations, namely, that which increases the amplitude of the unstable dark soliton. In this case, the instability scenario is *unbounded* in the framework of both the asymptotic equations (19) and (34) because these equations predict that the soliton velocity changes its sign in a finite time. This implies that a decrease of the minimum soliton intensity $I_{\min}$ cannot be suppressed by nonlinearity even in the vicinity of the insta-

bility threshold, and this leads to an essential transformation of the unstable dark soliton. The initial stage of this evolution corresponds to a decrease of the minimum intensity $I_{\min}$ until it reaches a value corresponding to a black soliton (at $v=0$), while the subsequent evolution depends on the global behavior of the nonlinear function $F(I)$ in the particular case of the GNLS equation (2). We investigate this phenomenon numerically in Secs. IV and V for some particular models. In addition, in Sec. VI we consider a very special type of dark soliton instability when both limiting cases of the dark soliton solutions ($v\to 0$ and $v\to c$) correspond to stable solitons, whereas there exists a narrow region of the soliton velocities v for which dark solitons become unstable. For such a special model, the unbounded scenario of the dark soliton evolution is not observed. We believe that the examples of the dark soliton instabilities discussed below display the most characteristic types of the instability-induced dynamics of dark solitons.

IV. COMPETING NONLINEARITIES

In the case of competing nonlinearities, e.g., focusing plus defocusing, the dark soliton solutions to Eq. (2) display features different from those for dark solitons of the conventional NLS equation. Due to self-focusing at smaller intensities of the cw background, the minimum amplitude of a dark soliton is nonzero even at $v=0$ for some values of the parameters. As a result, the total phase shift $S_s(v)$ and therefore the renormalized momentum $P_s(v)$ tend to zero in both limits $v\to 0$ and $v\to c$. This explains the appearance of a negative slope of the renormalized momentum $P_s(v)$ for small v and, correspondingly, leads to instability of dark solitons. For instance, this phenomenon is observed for the GNLS equation (2) with two competing power-law nonlinearities that have been considered in the theory of bright solitons (see, e.g., Ref. [20] and references therein)

$$F(I)=-\alpha I^{\sigma}+\beta I^{2\sigma}. \tag{40}$$

If α and β are both positive, the first term gives self-focusing [note the minus in front of $F(I)$ in Eq. (2)] and may prevent the existence of a black soliton with zero minimum intensity. For $\sigma=1$ the GNLS equation (2) with nonlinearity (40) corresponds to the focusing cubic and defocusing quintic nonlinearity and can describe a deviation from the Kerr medium of an optical material (see also the Introduction). Remarkably, the model (2) and (40) at $\sigma=1$ possesses an explicit solution for dark soliton. Therefore, although the general analysis of the competing nonlinearities is qualitatively correct for any value of σ, below we restrict ourselves by the case $\sigma=1$ when the results can be obtained in an analytic form.

The exact solution for a dark soliton of the cubic-quintic nonlinearity can be found in the form

$$\Phi^2(\xi)=1-\frac{2k^2}{a+b\cosh(2k\xi)}, \tag{41}$$

$$a=\left(\frac{4}{3}\beta-1\right), \quad b=\sqrt{a^2-\frac{4}{3}\beta k^2}, \tag{42}$$

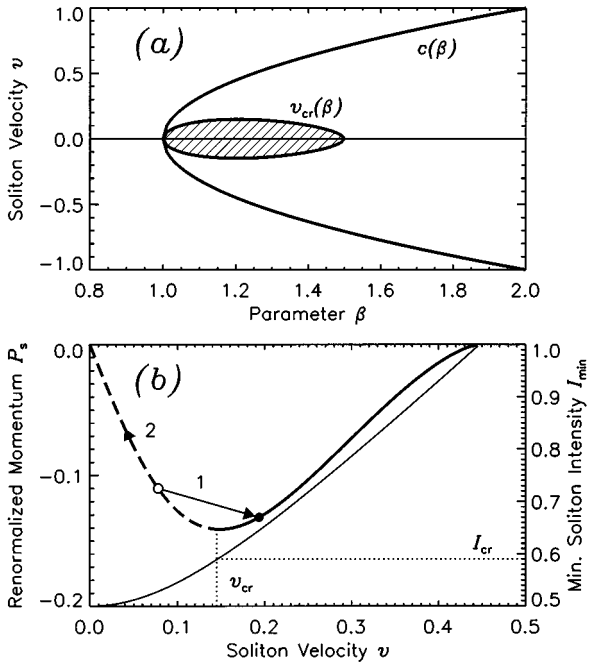

FIG. 3. (a) Regions of existence $|v|<c(\beta)$ and instability $|v|<v_{\rm cr}(\beta)$ of the dark soliton (41) and (42) and (b) renormalized momentum $P_s(v)$ for the dark soliton (41) and (42) at $\beta=1.2$. Thick dashed and solid branches correspond to unstable ($v<v_{\rm cr}$) and stable ($v>v_{\rm cr}$) dark solitons, respectively. The thin solid curve depicts the change of the minimum soliton intensity $I_{\min}$. Arrows 1 and 2 correspond to the evolution of the unstable soliton presented in Figs. 4 and 5, respectively.

where, for simplicity, we take $q=1$ and $\alpha=2$. The soliton amplitude k is defined by the soliton velocity v through the relation $k^2+v^2=\beta-1$.

First, we analyze the parameter region where the dark soliton (41) and (42) can exist. The condition $k^2>0$ yields $|v|<c(\beta)=\sqrt{\beta-1}$; see Fig. 3(a). Then we use the instability criterion defined above and calculate the slope of the function $P_s(v)$ to find the instability region: a dark soliton becomes unstable for $dP_s(v)/dv<0$. We have checked that the negative slope of $P_s(v)$ appears only for $1<\beta<1.5$, where the dark soliton at $v=0$ has a nonzero amplitude at the minimum $\Phi^2(0)=(3-2\beta)/\beta$. The function $P_s(v)$ for the particular case $\beta=1.2$ is shown in Fig. 3(b). Thus, for $1<\beta<1.5$ dark solitons in the cubic-quintic model become unstable for smaller velocities $0<|v|<v_{\rm cr}(\beta)$ and stable for larger velocities $v_{\rm cr}(\beta)<|v|<c(\beta)$. The instability region is shown in Fig. 3(a) as a dashed domain. As follows from this figure, the dark soliton (41) and (42) becomes unstable in a relatively small parameter domain and the critical value $v_{\rm cr}(\beta)$ does not exceed 0.145.

To study the evolution of an unstable dark soliton, we perform numerical simulations of Eq. (2) using, for better visualization, the equivalent solution for a (stationary) dark soliton on a moving cw background [see Eq. (6) at $k=v$]. We apply a small perturbation to change the amplitude of the dark soliton (41) and (42) adding a symmetric disturbance with small factor ϵ,

$$\psi_{\rm pert}(\xi)=\{\Phi(\xi)+\epsilon[1-\Phi^2(\xi)]\}e^{i\theta(\xi)},$$

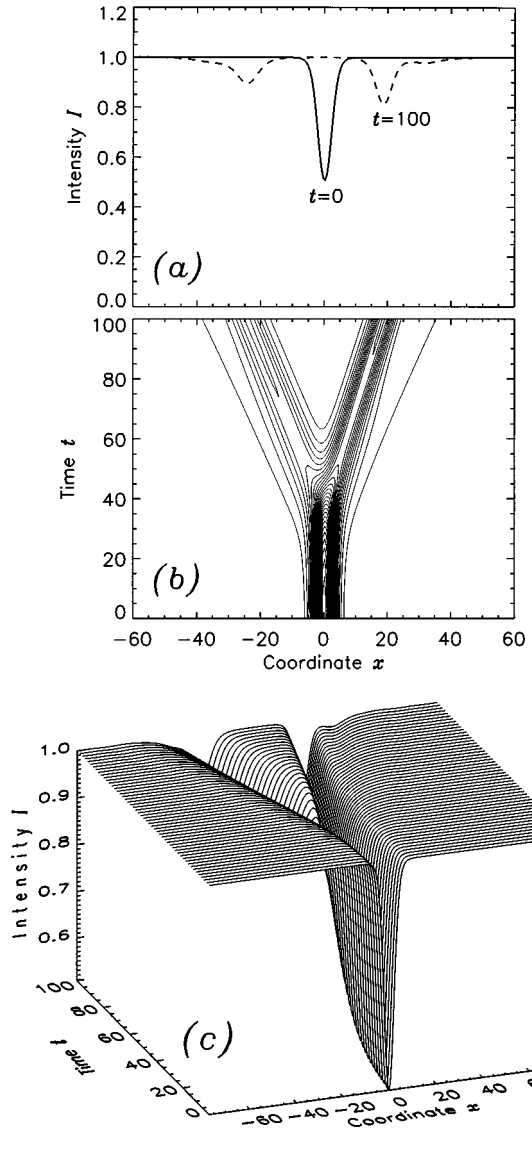

FIG. 4. Bounded scenario: Splitting of the unstable dark soliton (41) and (42) for $\beta=1.2$, $v_0=0.02$, and $\epsilon=+0.005$. Shown are (a) intensity profiles at $t=0$ (solid curve) and $t=100$ (dashed curve) and the corresponding (b) contour plot and (c) propagation dynamics.

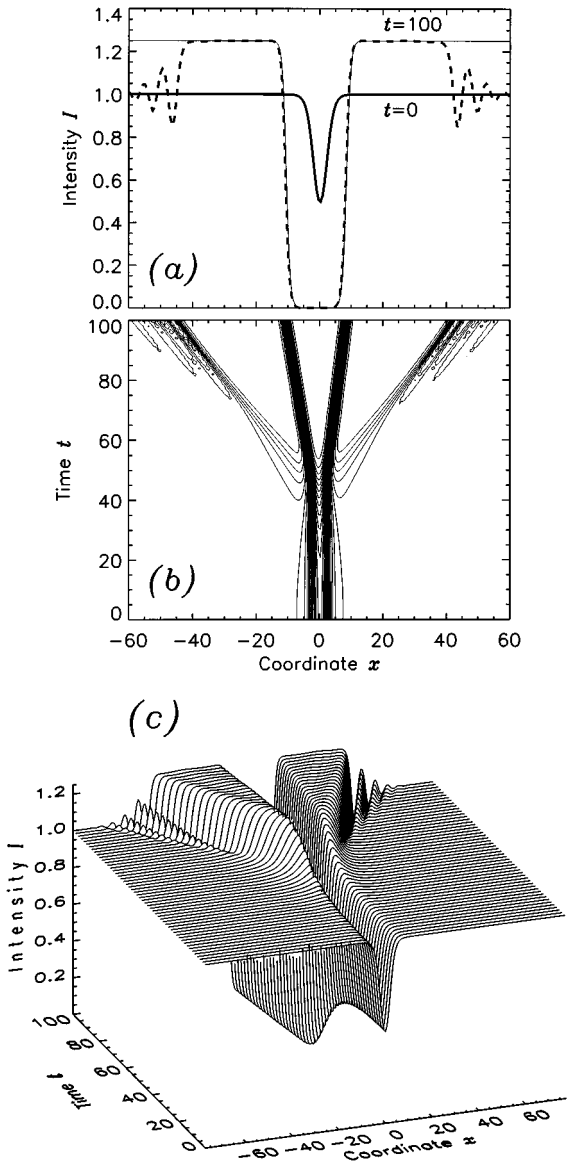

FIG. 5. Unbounded scenario: Collapse of the unstable dark soliton (41) and (42) into two kinks for $\beta=1.2$, $v_0=0.02$, and $\epsilon=-0.005$. Shown are (a) intensity profiles at $t=0$ (solid curve) and $t=100$ (dashed curve) and the corresponding (b) contour plot and (c) propagation dynamics. The thin solid curve in (a) presents, for a comparison, the exact kink solution (43).

which does not change the soliton phase. The initial velocity v_0 of the unstable soliton is chosen in the unstable region, while the amplitude ϵ is taken to be both positive and negative in the interval $0.0001<|\epsilon|<0.02$. The numerical simulations reveal two completely different scenarios of the dynamics of unstable dark solitons depending on the sign of the perturbation amplitude ϵ.

The first, bounded scenario is observed for $\epsilon>0$ when initially the soliton velocity is slightly increased. Effectively, this corresponds to a ''push'' of the unstable soliton toward the stable branch of $P_s(v)$ in Fig. 3(b) (curve 1) that exists for larger values of v. An example of such simulations is shown in Figs. 4(a)–4(c), where we clearly observe the soliton splitting, in accordance with the predictions of the analytic theory for a bounded scenario.

The second, unbounded scenario of the soliton instability takes place for $\epsilon<0$. In this case, the unstable dark soliton is pushed deeper into the instability region [see curve 2 in Fig. 3(b)]. The corresponding simulations are presented in Figs. 5(a)–5(c), where we observe the formation of two kinks (dashed curves) propagating in the opposite directions. We call this scenario of the soliton instability ''*collapse of dark solitons*,'' by an analogy with the well-known effect for bright solitons of certain types of GNLS equation (1).

Thus we can see that the dark solitons evolve asymmetrically, depending on the type of initial perturbation. To characterize the soliton evolution, in Fig. 6 we show the change of the minimum soliton intensity $I_{\min}$ for both scenarios [see Fig. 3(b)]. In the case of splitting ($\epsilon>0$), the initial exponential growth of the perturbation amplitude (upper solid curve) saturates at approximately $t=45$ and the unstable dark soliton splits into two stable solitons of smaller amplitudes (see curves 1 and 2 in Fig. 6), which move after the splitting

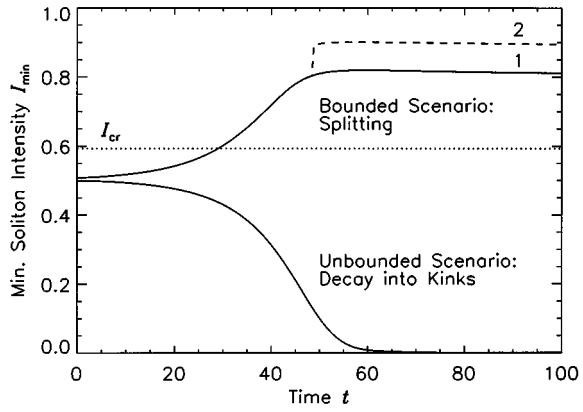

FIG. 6. Change of the minimum soliton intensity $I_{\min}$ for two scenarios of the soliton instability presented in Figs. 4 and 5: splitting (upper solid, 1, and dashed, 2, curves) and decay into kinks (collapse) (lower solid curve). The dotted line displays the critical intensity $I_{\rm cr}$, which corresponds to the instability threshold $v=v_{\rm cr}$ and it is defined in Fig. 3(b).

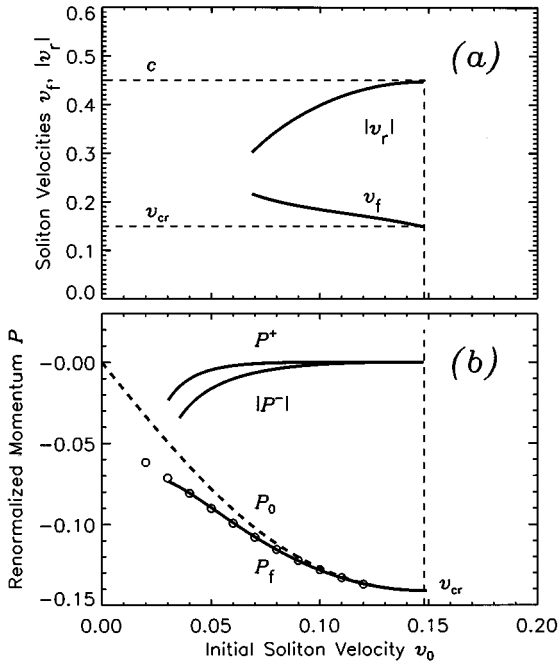

FIG. 7. (a) Analytical results for the velocities v_f and $|v_r|$ of two leading dark solitons created after the splitting vs the initial velocity v_0 of the unstable dark soliton. The dotted lines present the limit values $v=v_{\rm cr}$ and $v=c$. (b) Renormalized momenta of the final (largest) dark soliton P_f and the radiation fields $|P^{\pm}|$ vs the initial soliton velocity v_0, calculated analytically (solid curves) and numerically (open circles). The initial value of the renormalized momentum $P_0(v)$ is shown by a dashed curve and only its unstable branch $v_0 \leqslant v_{\rm cr}$ is displayed.

into opposite directions, as shown in Figs. 4(b) and 4(c). When the initial soliton velocity is selected far from the threshold value $v_{\rm cr}$, more than one secondary soliton is generated. In the case of decay into kinks ($\epsilon<0$), the exponential growth of the initial perturbation allows the minimum intensity to reach zero (see Fig. 6; lower solid curve). Then the region of zero intensity starts to spread out while the background intensity increases outside the localized wave [see Fig. 5(c)]. Finally, this process results in the formation of a new background of a special intensity $q_c=1.25$, instead of the initial value $q=1.0$, and in the steady-state propagation of two kinks. Such a kink is described by the exact solutions to the GNLS equations (1) and (40) at $\sigma=1$,

$$\Psi_k=\frac{\sqrt{q_c}}{\sqrt{1+e^{\pm\Delta}}}e^{i\omega_c t}, \tag{43}$$

where $q_c=3\alpha/4\beta$, $\Delta^2=\alpha q_c$, and $\omega_c=\frac{1}{6}\beta q_c^2$. The kink (43) connects two modulationally stable cw backgrounds, the background of the intensity q_c, and the zero-intensity background. For a comparison between the kinks generated due to the instability and the exact kink solution of the cubic-quintic model, we show the solutions (43) in Fig. 5(a) by thin solid curves, which are in excellent agreement with numerical results (thick dashed curves).

For the case of splitting of the unstable dark soliton, the velocities v_f and $|v_r|$ of the generated stable dark solitons can be evaluated analytically by means of the asymptotic theory. Indeed, the value v_f can be approximated as $v_f=v_0+\epsilon V_f$ [see Eq. (36)], while the value v_r is expressed through the effective KdV soliton amplitude κ, $|v_r|=c-\epsilon^2\kappa^2/2c$. To find the soliton parameter κ we use the assumption that the momentum P^- [see Eq. (39)] emitted by the perturbed dark soliton into the opposite direction corresponds to a novel dark soliton. In this case, the balance equation $P^-=192c\epsilon^3\kappa^3/(q\nu^2)$ defines the required value of the parameter κ. These results are presented in Fig. 7(a) as functions of the initial soliton velocity v_0.

Additionally, we calculate the contributions to the renormalized momentum from the final stable dark soliton P_f, the small-amplitude dark soliton P^-, and the perturbations of the continuous-wave background $P^+=P_0-P_f-P^-$ and present them in Fig. 7(b). The dashed curve depicts the momentum of the unstable dark solitons P_0, while the open circles show the numerical data for the momentum P_f of the (final) stable soliton. We note that the instability of the dark solitons in the case of competing nonlinearities always leads to a decrease of the soliton renormalized momentum (i.e., $P_f<P_0$). We have checked that this result is in agreement with the asymptotic prediction given by Eq. (37) because for the nonlinearity (40) the coefficient $K_s(v_0)$ is negative. On the other hand, the coefficient $\zeta_+(v_0)$ is negative for the values of v_0 close to $v_{\rm cr}$. This fact implies that the radiation field emitted in front of the perturbed dark soliton can lead to the *formation of an additional stable dark soliton*. Moreover, for smaller values of the velocity v_0, the coefficient ζ_+ becomes positive and the radiation field described by the function U^+ decays into dispersive waves. In any case, the part of the renormalized momentum P^+ that corresponds to radiation always remains small compared to the momentum P^- [see Fig. 7(b)]. This fact explains a decrease of the soliton renormalized momentum due to the dark soliton instability and also provides a clear observation of the splitting of the unstable dark solitons.

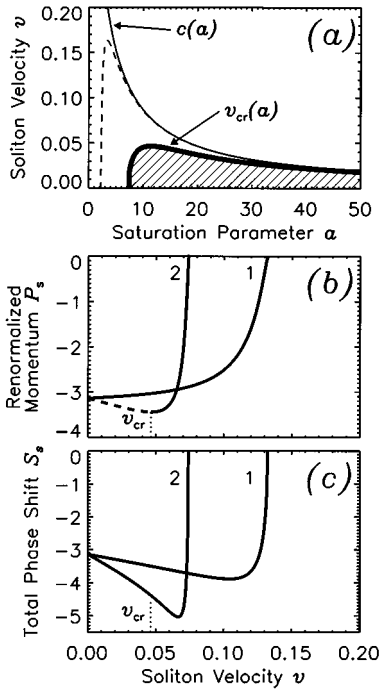

FIG. 8. (a) Regions of existence $v<c(a)$ and stability $v<v_{\rm cr}(a)$ of dark solitons in the saturable model (2) and (44) at $p=2$. The dashed curve depicts the region where a dark soliton has the total phase shift larger than π. Shown are (b) the renormalized momentum $P_s(v)$ and (c) the total phase shift $S_s(v)$ calculated for dark solitons at two values of the saturation parameter a: $a=6$ (curves 1) and $a=12$ (curves 2). The critical velocity $v_{\rm cr}$ corresponds to the instability threshold.

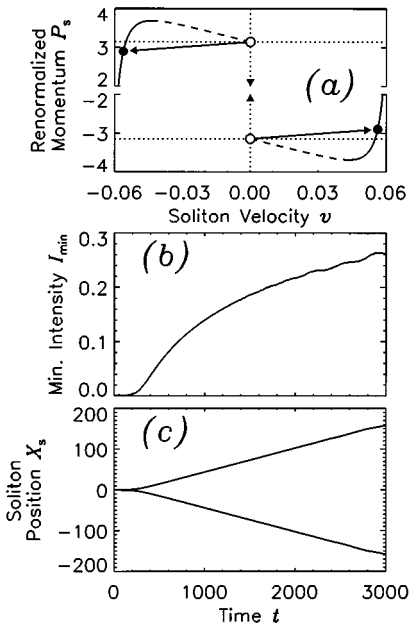

FIG. 9. Dynamics of an unstable black soliton in the model (2) and (44) at $p=2$ and $a=12$. Shown are (a) the renormalized momentum $P_s(v)$ and transitions corresponding to a transformation of an unstable ''black'' soliton into a stable ''gray'' soliton, (b) the change of the minimum soliton intensity $I_{\rm min}$, and (c) the change of the soliton position.

V. SATURABLE NONLINEARITY

In this section we consider the GNLS equation (2) with the generalized saturable nonlinearity $F(I)$ of the form

$$F(I)=1-\frac{1}{(1+aI)^p}, \tag{44}$$

where the parameter a has the meaning of a ratio of the maximum intensity $I_{\rm max}$ to the saturation intensity $I_{\rm sat}$, i.e., $a=I_{\rm max}/I_{\rm sat}$, and the parameter p is the saturation index. This type of nonlinearity in the GNLS equation (2) is used to analyze the effect of saturation of the nonlinear refractive index at larger intensities (see also the Introduction). In the case $p=1$ the nonlinearity (44) appears also in the theory of photovoltaic bright and dark solitons (see Refs. [18,19]). On the other hand, the model (2) and (44) at $p=2$ is known to exhibit soliton solutions in the form of bright and dark solitons [16]. With the help of these exact solutions, it has been recently revealed that dark solitons supported by the saturable nonlinearity may have the total phase shift larger than the limiting value π realized at the black soliton at $v=0$ [17]. However, later the instability of dark solitons has been pointed out exactly for the same model [26], but the relation between these two phenomena, i.e., larger-than-π soliton phase and instability, has not been established. Here we restrict our analysis to the simplest case $p=2$, which allows an analytic solution, but essentially the same dynamics of the dark soliton instabilities is observed as in the model (2) and (44) for other values of p.

First, in Fig. 8(a) we present the regions of existence $v<c(a)$ and instability $v<v_{\rm cr}(a)$ of the dark solitons in the model (2) and (44) at $p=2$ and $q=1$. Because of a symmetry, only positive values of the soliton velocity v are considered. The dashed line in Fig. 8(a) depicts the region of the parameter plane where the dark solitons have the total phase shift larger than π. The typical dependences of the renormalized momentum $P_s(v)$ and the total phase shift $S_s(v)$ are shown for $a=6$ and 12 in Figs. 8(b) and 8(c), respectively. It is clearly seen that the appearance of a large phase shift of the large-amplitude dark solitons serves as a pilot of their instability. However, among the dark solitons with the phase shift larger than π there exist both stable solitons, realized for larger velocities, and unstable solitons, realized for smaller velocities [see Fig. 8(a)].

Using the results of our asymptotic theory described in Sec. III B, we calculate the coefficients $K_s(v_0)$ and $\zeta_{\pm}(v_0)$ employing the exact solutions to the GNLS equation (2) with the saturable nonlinearity (44) at $p=2$. We find that the coefficient $K_s(v_0)$ is *always positive* and therefore the dark soliton instability due to a nonlinearity saturation should lead to an increase of the renormalized momentum according to Eq. (37). On the other hand, the coefficient $\zeta^+(v_0)$ is positive, i.e., the radiation in front of the perturbed dark soliton cannot lead to the creation of additional dark solitons, so that radiation always disperses. Moreover, our estimates show that this radiation should be dominant compared to the radia-

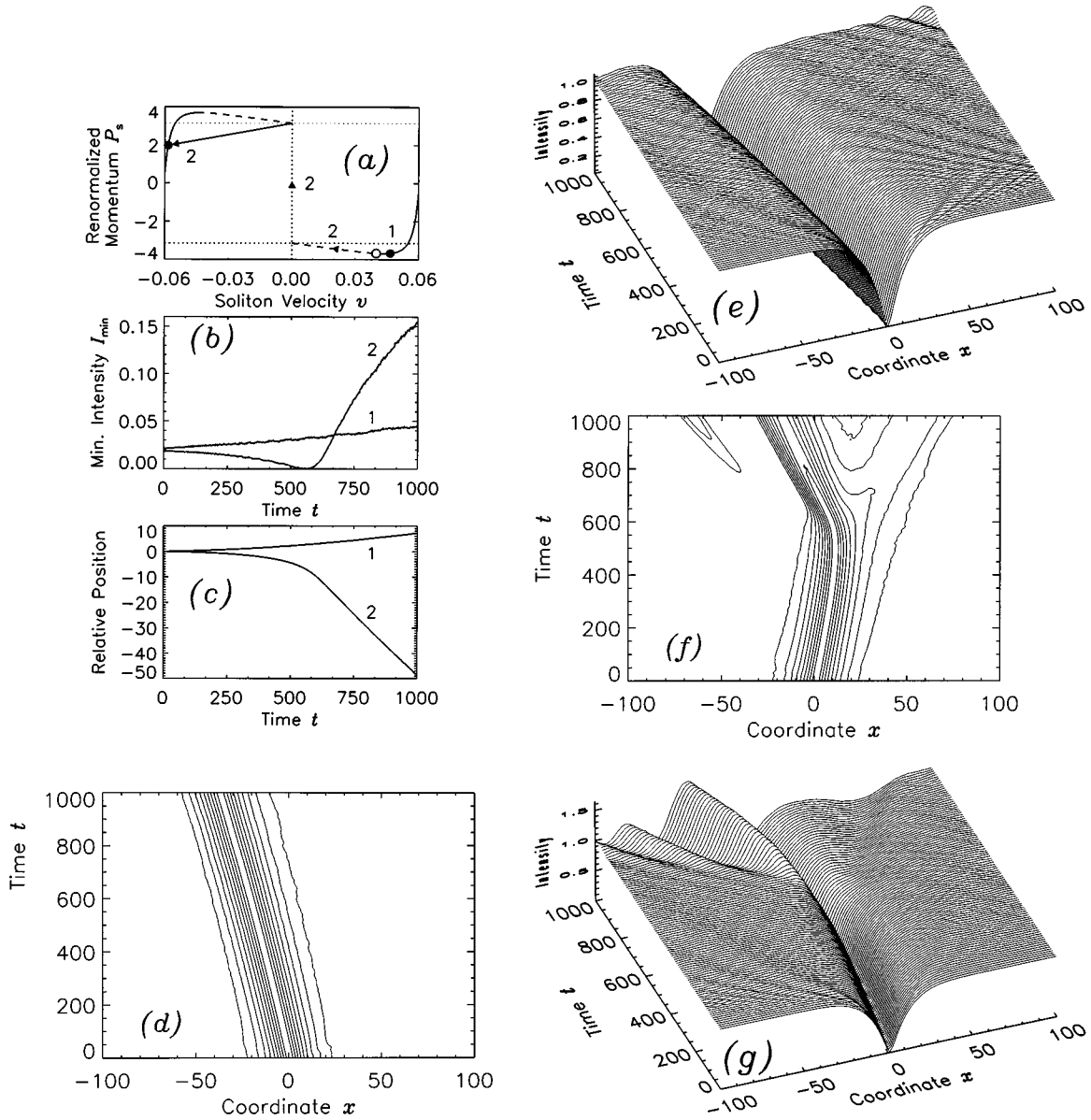

FIG. 10. Dynamics of an unstable gray soliton ($v_0 = 0.04$) in the model (2) and (44) at $p = 2$ and $a = 12$. Shown are (a) the renormalized momentum $P_s(v)$ and transitions corresponding to two types of the instability development, the change of (b) the minimum soliton intensity and (c) the relative soliton position for both scenarios, (d) and (f) contour plots, and (e) and (g) propagation dynamics corresponding to the bounded and unbounded scenarios, respectively.

tion moving in the opposite direction.

Next, we consider numerically the development of the dark soliton instability in the saturable model described by Eqs. (3) and (44) at $p = 2$. We find that the instability-induced soliton dynamics in this model displays features that are different from those mentioned in Sec. IV for the case of competing nonlinearities. As an initial condition, we consider two cases, a black soliton with $v_0 = 0$ and a gray soliton on a stationary background. A small perturbation to an unstable dark soliton is applied in the way already discussed for the case of competing nonlinearities (Sec. IV).

Figures 9(a)–9(c) correspond to the case of an initially unstable black soliton. Being pushed to either side by a small perturbation, the unstable black soliton transforms into a stable gray soliton that corresponds to a positive slope of the function $P_s(v)$ as shown in Fig. 9(a). The change of the soliton velocity is actually small for the nonlinearity (44) at $p = 2$, so that we show the change of the minimum soliton intensity [see Fig. 9(b)] and the soliton position [see Fig. 9(c)], which clearly indicate an initial, exponential growth of the perturbations upon the unstable black soliton and then its stabilization at the level that corresponds to a stable gray soliton.

The development of the instability of a gray soliton occurs basically in the same manner; see Figs. 10(a)–10(g). The different feature is asymmetric transitions for the positive ($\epsilon > 0$) and negative ($\epsilon < 0$) initial perturbations [see curves 1 and 2 in Fig. 10(a)]. An unstable gray soliton with an initially increased minimum amplitude $I_{\min}$ [curve 1 in Figs. 10(b) and 10(c)] slowly transforms into a stable soliton of larger velocity. The radiation emitted in front of and behind the unstable soliton is very small, but still can be seen in

Figs. 10(d) and 10(e), which display the contour plot and the propagation dynamics. On the other hand, the instability development of the gray soliton with an initially decreased minimum amplitude [curve 2 in Figs. 10(b) and 10(c)] occurs in two stages. At the first stage, the soliton changes almost adiabatically until its minimum amplitude reaches the zero value corresponding to a black soliton [see Fig. 10(b)]. The second stage is caused by the instability of the black soliton, the soliton undergoes a transition to the nearest stable gray soliton, which moves in the direction *opposite* the direction of the initial gray soliton [see Fig. 10(c)]. The contour plot presented in Fig. 10(f) and the propagation dynamics shown in Fig. 10(g) reveal that the radiation propagating in the opposite direction transforms to a dark soliton of a very small amplitude, according to the analytical theory. However, the generation of dispersive wave packets in front of the perturbed dark soliton dominates.

We note that the renormalized momentum of the perturbed dark soliton is greatly increased during this process. Such an increase of renormalized momentum of the dark soliton due to the instability development is related to a strong radiation in front of the dark soliton, which is in agreement with predictions of the asymptotic theory. This radiation is dominant compared to the other, soliton part of the radiation field and this fact makes the dark soliton splitting into two counterpropagating stable dark solitons difficult to investigate numerically (see also Fig. 3 in Ref. [26]).

VI. TRANSITING NONLINEARITY

In this section we consider one more example of the model of optical solitons described by the GNLS equation (2). It has been extensively discussed in connection with the phenomenon of the soliton bistability [11,12]. Soliton bistability can occur when unstable solitons are found for intermedite values of the soliton parameter (i.e., the propagation constant for bright solitons or velocity for dark solitons) allowing transitions between two (or more) types of solitons belonging to stable branches. One of the typical examples displaying this kind of phenomenon is the so-called *transiting nonlinearity*, which can be taken in the form [12]

$$F(I)=2I\{1+\alpha\tanh[\gamma(I^2-I_0^2)]\}. \tag{45}$$

The function (45) is a special case of the nonlinearity, which describes a smooth transition from one linear dependence for small intensities $I\ll I_0$, when $F(I)=2[1-\alpha\tanh(\gamma I_0^2)]I$, to the other linear dependence for large intensities $I\gg I_0$, when $F(I)\sim 2(1+\alpha)I$. Parameters α, I_0 in Eq. (45) characterize the amplitude and threshold intensity of the nonlinearity transition, while $\gamma^{-1/2}$ determines the characteristic width of the transition region.

The particular form (45) of the transiting nonlinearity has been introduced by Enns and Mulder [12] as a continuous approximation of the steplike model of the transiting nonlinearity introduced earlier by Kaplan in the theory of bistable bright solitons [11]. In particular, Enns and Mulder [12] have shown that the dependence of the complementary power $N_s(v)$ on the velocity of a dark soliton displays *three branches* and used this fact to introduce and characterize bistability of dark solitons. However, as follows from the asymptotic analysis we presented in Secs. II and III above, the soliton complementary power does not determine the stability of dark solitons. Thus the analysis of bistable dark solitons should be based on the soliton renormalized momentum.

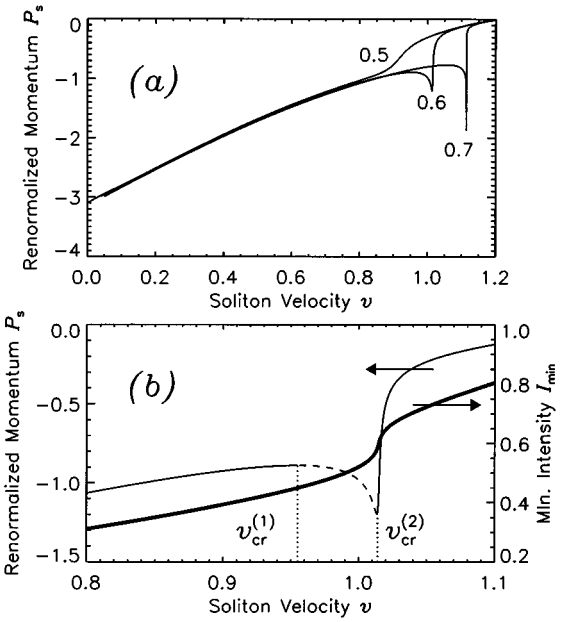

FIG. 11. (a) Renormalized momentum $P_s(v)$ for dark solitons supported by the transiting nonlinearity (45) for $\alpha=0.5$, $\gamma=10$, and different values of the parameter I_0: 0.5, 0.6, and 0.7, shown next to the curves. (b) Stable (thin solid) and unstable (dashed) branches of the soliton remormalized momentum $P_s(v)$ for the case $\alpha=0.5$, $\gamma=10$, and $I_0=0.6$. Thick solid curve displays a change of the minimum soliton intensity $I_{\min}$ vs soliton velocity v.

First, we calculate numerically the renormalized momentum $P_s(v)$ for dark solitons of the model (2) with the transiting nonlinearity (45) at $\alpha=0.5$, $\gamma=10$, and varying I_0. Some typical results are displayed in Fig. 11(a), where we can observe the appearence of a rather narrow region of the values of the soliton velocity (for some I_0), where the soliton renormalized momentum $P_s(v)$ displays *three branches* indicating a possibility of bistable dark solitons at a fixed value of the momentum.

In Fig. 11(b) we present an enlarged part of the dependence $P_s(v)$ at $I_0=0.6$ that displays stable (thin solid curve) and unstable (thin dashed curve) branches. The instability region $[v_{\rm cr}^{(1)}<v<v_{\rm cr}^{(2)}$, where, at $I_0=0.6$, $v_{\rm cr}^{(1)}\approx 0.955$ and $v_{\rm cr}^{(2)}\approx 1.014]$ is rather narrow and satisfies the criterion $\partial P_s(v)/\partial v<0$. It is obvious that the unstable branch corresponds to *gray solitons* of intermediate values of the minimum intensities $I_{\min}$ shown also in Fig. 10(b). Using the results of our asymptotic analysis, we expect that the evolution of unstable dark solitons would result in a transition (switching) from the unstable solution to one of the stable solutions with a greater or smaller value of the minimum intensities $I_{\min}$.

Numerical simulations of the instability-induced dynamics of dark solitons in the model (2) and (45) have been performed for a dark soliton with the intial velocity $v_0=0.96$ [see Figs. 12(a)–12(c)]. The dynamics displays in-

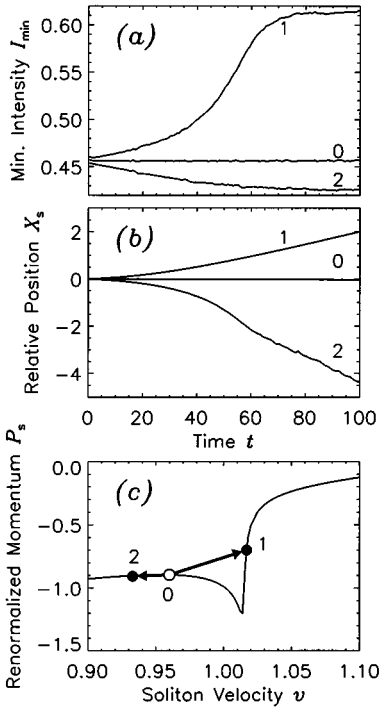

FIG. 12. Dynamics of the unstable dark soliton in the model (2) with the transiting nonlinearity (45) for $\alpha=0.5$, $\gamma=10$, and $I_0=0.6$. Soliton initial velocity $v_0=0.96$. Shown are (a) the evolution of the minimum soliton intensity $I_{\min}$ and (b) the change of the relative position of a soliton on a moving background, for both the unperturbed soliton (curves 0) and two types of the bounded scenario for the evolution of a perturbed dark soliton (curves 1 and 2). Transitions from the unstable branch to the stable branches (1 or 2) are shown in (c) by arrows on the plot of the renormalized momentum.

deed two types of transitions (switching) of a dark soliton from the unstable branch to one of the stable (marked as 1 or 2) branches of the stationary solutions. The first type of soliton switching describes a transition to a stable dark soliton with larger value of the minimum intensity $I_{\min}$ and larger velocity v [see curves 1 in Figs. 12(a)–12(c)]. The renormalized momentum of the unstable dark soliton increases as a result of this transition, as shown in Fig. 12(a). The second type of soliton switching describes a transition to another stable dark soliton, with a smaller value of the minimum intensity $I_{\min}$ and smaller velocity v [see curves 2 in Figs. 12(a)–12(c)]. In the latter case, the radiation in front of the dark soliton is negligible and, as a result, a change of the renormalized momentum of the unstable dark soliton is small, as shown in Fig. 12(c). Both types of soliton transitions are described by the bounded scenario for the evolution of the soliton velocity.

VII. CONCLUSION

We have presented, for the first time to our knowledge, a self-consistent analytical approach that describes the nonlinear regime of the evolution of unstable dark solitons in the framework of the generalized nonlinear Schrödinger equation. We have shown that, near the threshold of the soliton instability, both linear and nonlinear regimes of the instability-induced dynamics of dark solitons can be analyzed by the asymptotic multiscale expansion technique. This analytical approach gives us an effective tool of reducing the primary GNLS equation to asymptotic equations for the soliton parameters describing the evolution of the soliton velocity during the development of the (exponentially growing) linear instability and the subsequent nonlinear dynamics. Unlike the corresponding problem for bright solitons, radiation is shown to be very important in the instability-induced evolution of dark solitons and the development of the soliton instability is always accompanied by radiation, the effect being described by the same order of the asymptotic expansion. In particular, radiation fields may subsequently generate additional (shallow) dark solitons, so that our analytical results can also describe a splitting of an unstable dark soliton into stable dark solitons and radiation. Considering several examples of optical nonlinearities, we have demonstrated the most characteristic features of the instability-induced (bounded and unbounded) scenarios of the evolution of an unstable dark soltion. For example, in the case of the cubic-quintic nonlinearity, we have revealed ''collapse of dark solitons'' when an unstable dark soliton transforms into two diverging kinks. We believe that the analytical approach we have developed here and the basic types of instability scenarios we analyzed for particular models of optical nonlinearities are rather general to be useful for investigating instabilities of dark solitons in other nonlinear models.

Note added in proof. After submitting our manuscript for publication we became aware of several papers devoted to the analysis of linear instability of the so-called ''bubbles'' [V. G. Makhankov, *Soliton Phenomenology* (Kluwer, Dordrecht, 1990), pp. 270–272] in the GNLS equation with cubic-quintic nonlinearity which are, in fact, dark solitons with nonzero minimum intensity and no phase jump. More detailed analytical and numerical results for this case, including the criterion of the dark-soliton instability and collapse-like scenario, are presented in the recent paper by I. Barashenkov and E. Panova, Physica D **69**, 114 (1993).

APPENDIX A: FIRST-ORDER CORRECTION

Here we analyze the structure of the first-order perturbation correction ψ_1 induced by the slow evolution of an unstable dark soliton. Substituting the asymptotic multiscale expansion (17) into the GNLS equation (2), we obtain the linear problem for the function ψ_1,

$$\mathbf{L}\psi_1 \equiv \frac{d^2\psi_1}{d\xi^2} - 2iv\frac{d\psi_1}{d\xi} + [F(q) - F(|\psi_s|^2)]\psi_1 - F'(|\psi_s|^2) \times [\psi_s^2\psi_1^* + |\psi_s|^2\psi_1] = -2i\frac{dv}{dT}\frac{\partial\psi_s}{\partial v} + 2\frac{\partial R}{\partial T}\psi_s - 2i\frac{\partial R}{\partial X}\frac{d\psi_s}{d\xi}. \tag{A1}$$

First, we multiply this equation by $d\psi_s^*/d\xi$, integrate by parts with respect to ξ, and combine it with the complex

conjugated equation. As a result, we obtain a restriction on the parameter of the soliton velocity v,

$$\frac{dv}{dT}\frac{\partial P_s}{\partial v}=O(\epsilon), \tag{A2}$$

which gives the condition that the function ψ_1 is not exponentially diverging as $\xi\to\pm\infty$. (We have assumed here that the function $d\psi_s/d\xi$ tends to zero exponentially rapidly at infinity.) A general solution of Eq. (A1) can be found as a superposition of four eigenfunctions of the linear operator **L** and the corresponding forced solution due to the nonzero right-hand side of Eq. (A1). However, two eigenfunctions of the linear operator **L** lead to a trivial renormalization of the soliton parameters v and R, while the third one is exponentially diverging. Therefore, to obtain *a localized solution* for ψ_1 we take into account only one *nontrivial* eigenfunction of the linear operator **L** and then rewrite the solution to Eq. (A1) at the inner interval, where $\xi\sim O(1)$ and $X\to X_s(T)$, in the form

$$\psi_1=\frac{dv}{dT}\tilde{\psi}_1(\xi;v,q)+iQ_s\xi\psi_s-\left(Q_s+\frac{\partial R_s}{\partial X}\right)\frac{\partial\psi_s}{\partial v}+\frac{q}{c^2}\left(vQ_s-\frac{\partial R_s}{\partial T}\right)\frac{\partial\psi_s}{\partial q}, \tag{A3}$$

where we used the notations

$$Q_s\equiv Q|_{X=X_s},\quad R_s=R|_{X=X_s},$$

$Q(X,T)$ being the amplitude of the localized eigenfunction. The function $\tilde{\psi}_1$ cannot be written in an explicit form. However, it follows from Eq. (A1) that the real and imaginary parts of this function have symmetries opposite those of the real and imaginary parts of the function ψ_s. As a result, the function $\tilde{\psi}_1$ does not produce any contribution in the results of the subsequent analysis.

Now we consider the asymptotic values of the functions ψ_s and ψ_1 at infinities, which we denote as

$$\psi_{s\infty}^{\pm}=\lim_{\xi\to\pm\infty}\psi_s=\sqrt{q}e^{\pm(i/2)S_s},\quad \psi_{1\infty}^{\pm}=\lim_{\xi\to\pm\infty}\psi_1.$$

To calculate the values $\psi_{1\infty}^{\pm}$ explicitly, we rewrite Eq. (A1) for $\xi\to\pm\infty$,

$$\frac{d^2\psi_{1\infty}^{\pm}}{d\xi^2}-2iv\frac{d\psi_{1\infty}^{\pm}}{d\xi}-2c^2[\psi_{1\infty}^{\pm}+e^{\pm iS_s}\psi_{1\infty}^{\pm *}]=2\left(\frac{\partial R}{\partial T}\pm\frac{1}{2}\frac{\partial S_s}{\partial v}\frac{dv}{dT}\right)\psi_{s\infty}^{\pm}, \tag{A4}$$

where S_s and c are given by (10) and (16). Equation (A4) has a simple solution

$$\psi_{1\infty}^{\pm}=i(Q\pm d)\xi\psi_{s\infty}^{\pm}+\frac{i(w\pm W)}{2\sqrt{q}\sin(S_s/2)}, \tag{A5}$$

where $d(T)$, $w(T)$, and $W(X,T)$ are the parameters that satisfy two constraints

$$vQ-\frac{\partial R}{\partial T}=\frac{c^2}{q}W, \tag{A6}$$

$$vd-\frac{1}{2}\frac{\partial S_s}{\partial v}\frac{dv}{dT}=\frac{c^2}{q}w. \tag{A7}$$

The system (A6) and (A7) is not closed because the parameters d and w should be expressed through the velocity of the perturbed dark soliton. To close the system, we use the balance equation for density of the power n, which follows from the GNLS equation (2),

$$\frac{\partial n}{\partial t}=\frac{\partial k}{\partial x}, \tag{A8}$$

where

$$n=\frac{1}{2}(|\psi|^2-q),\quad k=\frac{i}{4}\left(\psi^*\frac{\partial\psi}{\partial x}-\frac{\partial\psi^*}{\partial x}\psi\right). \tag{A9}$$

Then we rewrite Eq. (A8) with new variables ξ, X, and T and integrate it with respect to ξ. As a result, in the first-order approximation the power balance equation (A8) reduces to the relation

$$\frac{v}{2}(\psi_{s\infty}\psi_{1\infty}^*+\psi_{s\infty}^*\psi_{1\infty})\Big|_{-\infty}^{+\infty}+\frac{i}{4}\left(\psi_{s\infty}^*\frac{\partial\psi_{1\infty}}{\partial\xi}-\psi_{s\infty}\frac{\partial\psi_{1\infty}^*}{\partial\xi}\right)\Bigg|_{-\infty}^{+\infty}=\frac{\partial N_s}{\partial v}\frac{dv}{dT}, \tag{A10}$$

where the symbol $Z|_{-\infty}^{+\infty}$ stands for a difference (Z^+-Z^-). Equation (A10) closes the system (A6) and (A7) and allows us to express the parameters d and w through the first-order derivative of the soliton velocity v as

$$d=-\frac{1}{(c^2-v^2)}\left[\frac{c^2}{q}\frac{\partial N_s}{\partial v}+\frac{v}{2}\frac{\partial S_s}{\partial v}\right]\left(\frac{dv}{dT}\right), \tag{A11}$$

$$w=-\frac{1}{(c^2-v^2)}\left[v\frac{\partial N_s}{\partial v}+\frac{q}{2}\frac{\partial S_s}{\partial v}\right]\left(\frac{dv}{dT}\right). \tag{A12}$$

APPENDIX B: DERIVATION OF ASYMPTOTIC EQUATIONS

Here we analyze the equations for the momentum and energy, which follow from the GNLS equation (2), and derive the asymptotic equations governing the instability-induced evolution of the soliton velocity $v(T)$. The balance equations for the GNLS equation (2) can be written in the form

$$\frac{\partial p}{\partial t}=\frac{\partial o}{\partial x},\quad \frac{\partial h}{\partial t}=\frac{\partial g}{\partial x}, \tag{B1}$$

where p and h are the densities of the renormalized momentum and Hamiltonian and o and g are the corresponding generalized flows. They are given by the expressions

$$p=\frac{i}{2}\left(\psi^*\frac{\partial\psi}{\partial x}-\psi\frac{\partial\psi^*}{\partial x}\right)\left(1-\frac{q}{|\psi|^2}\right), \tag{B2}$$

$$h=\frac{1}{2}\left|\frac{\partial\psi}{\partial x}\right|^2+\frac{1}{2}\int_q^{|\psi|^2}[F(I)-F(q)]dI, \tag{B3}$$

$$o=-\frac{1}{4}\left(\psi^*\frac{\partial^2\psi}{\partial x^2}+\psi\frac{\partial^2\psi^*}{\partial x^2}\right)\left(1-\frac{q}{|\psi|^2}\right)+\frac{1}{2}\left|\frac{\partial\psi}{\partial x}\right|^2 -\frac{1}{2}\int_q^{|\psi|^2}F(I)dI+\frac{1}{2}F(|\psi|^2)(|\psi|^2-q), \tag{B4}$$

$$g=\frac{i}{4}\left(\frac{\partial\psi^*}{\partial x}\frac{\partial^2\psi}{\partial x^2}-\frac{\partial\psi}{\partial x}\frac{\partial^2\psi^*}{\partial x^2}\right)+\frac{i}{4}[F(q)-F(|\psi|^2)] \times\left(\psi\frac{\partial\psi^*}{\partial x}-\psi^*\frac{\partial\psi}{\partial x}\right). \tag{B5}$$

Now we express the balance equations (B1)–(B5) with new variables ξ, X, and T and then integrate them with respect to ξ. As a result, in the second-order approximation, the equation for the momentum leads to an ordinary differential equation

$$\frac{1}{\epsilon}\frac{dP}{dT}=2\left(w-\frac{qv}{c^2}d\right)\left(vQ_s-\frac{\partial R_s}{\partial T}\right)+2(qd-vw) \times\left(Q_s+\frac{\partial R_s}{\partial X}\right). \tag{B6}$$

Here the derivative d/dT is evaluated in the reference frame of the moving soliton

$$\frac{d}{dT}=\left(\frac{\partial}{\partial T}+v\frac{\partial}{\partial X}\right)\Bigg|_{X=X_s(T)}$$

and P is the renormalized momentum of the perturbed dark soliton

$$P=\int_{-\infty}^{+\infty}p\ d\xi=P_s(v,q)+\epsilon\delta P, \tag{B7}$$

where

$$\delta P=\frac{q}{c^2}\left(vQ_s-\frac{\partial R_s}{\partial T}\right)\left(\frac{\partial P_s}{\partial q}-S_s\right)-\left(Q_s+\frac{\partial R_s}{\partial X}\right) \times\left(\frac{\partial P_s}{\partial v}+2N_s\right).$$

On the other hand, the balance equation for Hamiltonian leads to the second differential equation

$$\frac{1}{\epsilon}\frac{dH}{dT}=2(vw-qd)\left(vQ_s-\frac{\partial R_s}{\partial T}\right)+2(qvd-c^2w) \times\left(Q_s+\frac{\partial R_s}{\partial X}\right). \tag{B8}$$

H is the renormalized Hamiltonian of the GNLS equation calculated for the perturbed dark soliton

$$H=\int_{-\infty}^{+\infty}h\ d\xi=H_s(v,q)+\epsilon\delta H, \tag{B9}$$

where

$$\delta H=-\frac{vq}{c^2}\left(vQ_s-\frac{\partial R_s}{\partial T}\right)\left(\frac{\partial P_s}{\partial q}-S_s\right)+v\left(Q_s+\frac{\partial R_s}{\partial X}\right) \times\left(\frac{\partial P_s}{\partial v}+2N_s\right).$$

APPENDIX C: RADIATION FIELDS

Here we present a more detailed analysis of the asymptotic expansion (18) valid outside the soliton region. To do so, we substitute this expansion into the GNLS equation (2) and derive a relation between the components of the radiation fields,

$$U^{\pm}=-\frac{q}{c^2}\frac{\partial\Theta_0^{\pm}}{\partial T}, \tag{C1}$$

where two functions $\Theta_0^{\pm}(X,T)$ obey the standard scalar wave equations

$$\frac{\partial^2\Theta_0^{\pm}}{\partial T^2}-c^2\frac{\partial^2\Theta_0^{\pm}}{\partial X^2}=0. \tag{C2}$$

The general solution to either of the wave equations (C2) can be presented as a superposition of two counterpropagating waves moving with the finite speed c. Since the dark soliton propagates with the velocity v, which is less than the limiting speed c of linear waves $|v|<c$, the radiation field in front of the dark soliton is presented by the wave propagating to the right, while the radiaton behind the dark soliton moves to the left (see Fig. 1). In other words, $\Theta_0^{\pm}=\Theta_0^{\pm}(X\mp cT)$ and the relations (C1) can be rewritten as

$$U^{\pm}=\pm\frac{q}{c}\frac{\partial\Theta_0^{\pm}}{\partial X}. \tag{C3}$$

These relations are valid everywhere on the axis X including the soliton region $X\to X_s(T)$. On the other hand, in Appendix A we have found the asymptotic values $\psi_{1\infty}^{\pm}$ for the first-order correction ψ_1 as $\xi\to\pm\infty$ [see Eq. (A5)]. Therefore, using the expansions (17) and (18) and the matching condition $\epsilon\xi=X-X_s(T)$, we can evaluate the values $U^{\pm}$ and $\partial\Theta_0^{\pm}/\partial X$ for $\xi\to\pm\infty$ and $X\to X_s(T)$,

$$U^{\pm}\to W_s\pm w,\ \frac{\partial\Theta_0^{\pm}}{\partial X}\to Q_s+\frac{\partial R_s}{\partial X}\pm d, \tag{C4}$$

where $W_s\equiv W|_{X=X_s}$. Then, using the relations (C3) and (A6), we express the functions Q_s and R_s through the derivative of the velocity $v(T)$ of the perturbed dark soliton

$$vQ_s-\frac{\partial R_s}{\partial T}=cd, \tag{C5}$$

$$Q_s+\frac{\partial R_s}{\partial X}=\frac{c}{q}w. \tag{C6}$$

Finally, we note that, by extending the asymptotic expansion (18) into higher orders, we can also describe nonlinear

and dispersive effects for the evolution of the radiation fields. However, in order to take both effects in the same order of the asymptotic expansion, we have to reorder the multiscale expansion according to the transformation

$$U^{\pm} \to \epsilon U^{\pm}(X \mp cT, \tau),$$

where $\tau = \epsilon^3 t$. Then, straightforward calculations reveal (see also [1,27]) that the long-term evolution of the radiation fields $U^{\pm}(X,\tau)$ obeys two uncoupled KdV equations

$$\mp 8c \frac{\partial U^{\pm}}{\partial \tau} - \nu U^{\pm} \frac{\partial U^{\pm}}{\partial X} + \frac{\partial^3 U^{\pm}}{\partial X^3} = 0, \tag{C7}$$

where $\nu = 2[3F'(q) + qF''(q)]$.

[1] Yu.S. Kivshar, IEEE J. Quantum Electron. **28**, 250 (1993).

[2] V.E. Zakharov and A.B. Shabat, Zh. Éksp. Teor. Fiz. **64**, 1672 (1973) [Sov. Phys. JETP **37**, 923 (1973)].

[3] A. Hasegawa and F. Tappert, Appl. Phys. Lett. **23**, 171 (1973).

[4] B. Luther-Davies and X. Yang, Opt. Lett. **17**, 496 (1992); **17**, 1755 (1992).

[5] G.A. Swartzlander, Jr., D.R. Andersen, J.J. Regan, H. Yin, and A.E. Kaplan, Phys. Rev. Lett. **66**, 1583 (1991).

[6] G.R. Allan, S.R. Skinner, D.R. Andersen, and A.L. Smirl, Opt. Lett. **16**, 156 (1991).

[7] B. Luther-Davies, R. Powles, and V. Tikhonenko, Opt. Lett. **19**, 1816 (1994).

[8] M. Taya, M.C. Bashaw, M.M. Fejer, M. Segev, and G.C. Valley, Phys. Rev. A **52**, 3095 (1995).

[9] M. Nakazawa and K. Suzuki, Electron. Lett. **31**, 1076 (1995); **31**, 1084 (1995).

[10] V.E. Zakharov, V.V. Sobolev, and V.S. Synakh, Zh. Éksp. Teor. Fiz. **60**, 136 (1971) [Sov. Phys. JETP **33**, 77 (1971)]; V.E. Zakharov and V.S. Synakh, *ibid.* **68**, 940 (1975) [*ibid.* **41**, 465 (1975)].

[11] A.E. Kaplan, Phys. Rev. Lett. **55**, 1291 (1985); IEEE J. Quantum Electron. **21**, 1538 (1985).

[12] R.H. Enns and L.J. Mulder, Opt. Lett. **14**, 509 (1989); L.J. Mulder and R.H. Enns, IEEE J. Quantum Electron. **25**, 2205 (1989).

[13] S. Gatz and J. Herrmann, J. Opt. Soc. Am. B **8**, 2296 (1991); Opt. Lett. **17**, 484 (1992); J. Herrmann, Opt. Commun. **91**, 337 (1992).

[14] F.G. Bass, V.V. Konotop, and S.A. Puzenko, Phys. Rev. A **46**, 4185 (1992).

[15] A.W. Snyder and A.P. Sheppard, Opt. Lett. **18**, 499 (1993).

[16] W. Krolikowski and B. Luther-Davies, Opt. Lett. **18**, 188 (1993).

[17] W. Krolikowski, N. Akhmediev, and B. Luther-Davies, Phys. Rev. E **48**, 3980 (1993).

[18] G.C. Valley, M. Segev, B. Crosignani, A. Yariv, M.M. Fejer, and M.C. Bashaw, Phys. Rev. A **50**, R4457 (1994).

[19] D.N. Christodoulides and M.I. Carvalho, J. Opt. Soc. Am. B **12**, 1628 (1995). This paper deals with the so-called steady-state photorefractive screening solitons, which, unlike the photovoltaic solitons discussed in Ref. [18], require more complicated boundary conditions. Nevertheless, the main physical effects are similar to the case of saturable nonlinearity; see also M. Segev, G.C. Valley, B. Crosignani, P.DiPorto, and A. Yariv, Phys. Rev. Lett. **73**, 3211 (1994).

[20] D.E. Pelinovsky, V.V. Afanasjev, and Yu.S. Kivshar, Phys. Rev. E **53**, 1940 (1996).

[21] P. Roussignol, D. Ricard, J. Lukasik, and C. Flytzanis, J. Opt. Soc. Am. B **4**, 5 (1987); L.H. Acioli, A.S.L. Gomes, J.M. Hickmann, and C.B. de Araujo, Appl. Phys. Lett. **56**, 2279 (1990); F. Lederer and W. Biehlig, Electron. Lett. **30**, 1871 (1994).

[22] B. Lawrence, M. Cha, W.E. Torruellas, G.I. Stegeman, S. Etemad, G. Baker, and F. Kajzer, Appl. Phys. Lett. **64**, 2773 (1994); B. Lawrence, W.E. Torruellas, M. Cha, M.L. Sundheimer, G.I. Stegeman, J. Meth, S. Etemad, and G. Baker, Phys. Rev. Lett. **73**, 597 (1994).

[23] J.L. Coutaz and M. Kull, J. Opt. Soc. Am. B **8**, 95 (1991).

[24] T.K. Gustafson, P.L. Kelley, R.Y. Chiao, and R.G. Brewer, Appl. Phys. Lett. **12**, 165 (1968); J.D. Reichert and W.G. Wagner, IEEE J. Quantum Electron. **QE-4**, 221 (1968); J.H. Margurger and E. Dawes, Phys. Rev. Lett. **21**, 556 (1968).

[25] E. A. Kuznetsov, A. M. Rubenchik, and V. E. Zakharov, Phys. Rep. **142**, 103 (1986).

[26] Yu.S. Kivshar and W. Krolikowski, Opt. Lett. **20**, 1527 (1995).

[27] Yu.S. Kivshar, D. Anderson, and M. Lisak, Phys. Scr. **47**, 679 (1993).

[28] Yu.S. Kivshar and X. Yang, Phys. Rev. E **49**, 1657 (1994).

[29] Yu.S. Kivshar and W. Krolikowski, Opt. Commun. **114**, 353 (1995).

[30] Yu.S. Kivshar and B.A. Malomed, Rev. Mod. Phys. **61**, 763 (1989).

[31] D.E. Pelinovsky, Yu.A. Stepanyants, and Yu.S. Kivshar, Phys. Rev. E **51**, 5016 (1995).

[32] We note that the definition of the renormalized momentum given in Eq. (8) differs by the sign in front of the integral from that used in Ref. [26].

[33] M.J. Ablowitz and H. Segur, *Solitons and the Inverse Scattering Transform* (SIAM, Philadelphia, 1981).